Highly specialized carbohydrate metabolism capability in *Bifidobacterium* strain associated with intestinal barrier maturation in early preterm infants

Bing Ma,[a,b] Sripriya Sundararajan,[c] Gita Nadimpalli,[d] Michael France,[a,b] Elias McComb,[a] Lindsay Rutt,[a] Jose M Lemme-Dumit,[c,e] Elise Janofsky,[c] Lisa S. Roskes,[c] Pawel Gajer,[a,b] Li Fu,[a] Hongqiu Yang,[a] Mike Humphrys,[a] Luke J Tallon,[a] Lisa Sadzewicz,[a] Marcela F Pasetti,[b,c,e] Jacques Ravel,[a,b] Rose M Viscardi[c]

[a]Institute for Genome Sciences, University of Maryland School of Medicine, Baltimore, USA

[b]Department of Microbiology and Immunology, University of Maryland School of Medicine, Baltimore, USA

[c]Department of Pediatrics, University of Maryland School of Medicine, Baltimore, USA

[d]Department of Epidemiology, University of Maryland School of Medicine, Baltimore, USA

[e]Center for Vaccine Development and Global Health, University of Maryland School of Medicine, Baltimore, USA

Address correspondence to Bing Ma, bma@som.umaryland.edu

ABSTRACT “Leaky gut”, or high intestinal barrier permeability, is common in preterm newborns. The role of microbiota in this process remains largely uncharacterized. We employed both short- and long-read sequencing of the 16S rRNA gene and metagenomes to characterize the intestinal microbiome of a longitudinal cohort of 113 preterm infants born between $24^{0/7}$-$32^{6/7}$ weeks of gestation. Enabled by enhanced taxonomic resolution, we found significantly increased abundance of *Bifidobacterium breve* and a diet rich in mother’s breastmilk to be associated with intestinal barrier maturation during the first week of life. We combined these factors using genome-resolved metagenomics and identified a highly specialized genetic capability of the *Bifidobacterium* strains to assimilate human milk oligosaccharides and host-derived glycoproteins. Our study proposed mechanistic roles of breastmilk feeding and intestinal microbial colonization in postnatal intestinal barrier maturation; these observations are critical towards advancing therapeutics to prevent and treat hyperpermeable gut-associated conditions, including necrotizing enterocolitis.

IMPORTANCE Despite improvements in neonatal intensive care, necrotizing enterocolitis (NEC) remains a leading cause of morbidity and mortality. "Leaky gut", or intestinal barrier immaturity with elevated intestinal permeability, is the proximate cause of susceptibility to NEC. Early detection and intervention to prevent leaky gut in “at-risk” preterm neonates is critical to lower the risk for potentially life-threatening complications like NEC. However, the complex interactions between the developing gut microbial community, nutrition, and intestinal barrier function, remain largely uncharacterized. In this study, we revealed the critical role of sufficient breastmilk feeding volume and specialized carbohydrate metabolism capability of *Bifidobacterium* in coordinated postnatal improvement of intestinal barrier. Determining the clinical and microbial biomarkers that drive the intestinal developmental disparity will inform early detection and novel therapeutic strategies to promote appropriate intestinal barrier maturation, prevent NEC and other adverse health conditions in preterm infants.

KEYWORDS preterm infant; gut microbiome; leaky gut; intestinal barrier maturation; human milk oligosaccharides; *Bifidobacterium*

Early preterm neonates are particularly vulnerable to life-threatening events and routinely require intensive care and medical intervention to survive (1). The physiological immaturity of their gastrointestinal (GI) tract is commonly associated with deficiencies in barrier functions that result in a clinical syndrome known as “leaky gut” (2-5). Under leaky gut condition, the bacteria and bacterial products normally confined to the intestinal lumen are able to translocate into the peripheral circulation through the hyperpermeable epithelial barrier, which could lead to widespread invasion of the intestinal epithelium and gut lamina propria, mucosal inflammation, epithelial cell damage, intestinal necrosis, systemic infection, and ultimately multi-organ failure and death (4, 6, 7). Necrotizing enterocolitis (NEC) is a prominent bacterial translocation-associated GI condition that affects 7-10% of preterm neonates or 1-5% of all neonatal NICU admissions with a devastating mortality rate as high as 50% (8-12). Early detection of an aberrant leaky gut and early intervention to limit intestinal injury are of paramount importance to reduce the incidence of subsequent complications including NEC (12, 13).

A functional intestinal barrier combines a physical barrier that encompasses chemical, immunological and microbiological components (14). We and others have found that the first week of life (day 8±2 post-birth) is a critical window during which the most rapid postnatal intestinal maturation occurs (15-17). More importantly, these earlier studies demonstrated that the intestinal barrier function, which develops mostly *in utero* in term infants, can be improved postnatally. They also showed that the intestinal barrier maturation does not occur at the same rate, with ~40% of preterm neonates (<33 weeks gestation) failing to develop a functional intestinal barrier within the first two weeks of life (15, 16). Determining the factors that drive this developmental

disparity will inform early detection and novel therapeutic strategies to promote intestinal barrier maturation.

Efforts to characterize the microbiological factors that are associated with intestinal barrier maturation have thus far yielded unsatisfactory results (18). There are no microbial biomarkers predictive of intestinal development. A major limitation is the use of partial 16S rRNA gene sequences to evaluate the taxonomic composition of gut microbiota. The short sequences lack the phylogenetic signal necessary to describe taxonomic composition at species or even genus level. Many of the PCR primers used to amplify variable regions of the 16S rRNA gene fail to amplify members of the genus *Bifidobacterium* (19-21). *Bifidobacterium* species are known to be frequent colonizers of infant guts (22), and are considered to play beneficial roles in intestinal development and influence maturation of the neonatal gut, potentially through stimulating colonic epithelial proliferation, modulation of host defense responses and protection against bacterial infections (23, 24). To investigate *Bifidobacterium* and other bacterial groups predictive of early intestinal development and maturation are of pivotal importance.

In this study, we sought to characterize the role of early assembly of infant gut microbiota and its metabolism in postnatal intestinal barrier maturation. We build upon the results of past studies (15, 16) using an expanded cohort (N=113) of early preterm neonates ($24^{0/7}$-$32^{6/7}$ weeks of gestation) from whom stool samples were collected daily up to 21 days post birth. High resolution approaches were applied to characterize the composition of the developing gut microbiota with substantially enhanced taxonomic resolution including *Bifidobacterium* species, which we identified as the microbial biomarker associated with postnatal intestinal barrier maturation within the first week of

life. Whole community metagenomes using both short- and long-read sequences provided a detailed characterization of the genetic content of these *Bifidobacterium* species, which were shown to have distinct genetic features affording complete carbohydrate foraging capabilities, including human milk oligosaccharides (HMOs) and host-derived glycoprotein. The presence of specific strains of *Bifidobacterium* may inform the early detection of aberrant intestinal permeability. Supplementation of these bifidobacterial strains could be leveraged in novel intervention strategies for the prevention of leaky gut and its devastating sequelae in preterm newborns.

RESULTS

Clinical cohort. We examined a prospective cohort of 113 preterm infants $24^{0/7}$-$32^{6/7}$ weeks of gestation including 37 subjects described in a previous analysis (**Table S1**). Fecal samples were collected daily until postnatal day 21 or discharge from the Neonatal Intensive Care Unit (NICU, **Fig. 1**). Mean gestational age (GA) of infants at birth was 29.9±2.3 weeks. A total of 28 infants (24.8%) were <28 weeks GA, and 85 (75.2%) were $28^{0/7}$-$32^{6/7}$ weeks GA. The mean birth weight was 1,381g (±415g); 66 (58.4%) newborns were classified as very low birth weight (VLBW, <1,500g birth weight) and 26 (23.0%) were classified as extremely low birth weight (ELBW, <1,000g).

Intestinal permeability (IP) was determined 7-10 days post-birth when rapid intestinal barrier maturation normally takes place (15, 16). IP was calculated as the ratio of two enterally administered sugar probes Lactulose (La) and Rhamnose (Rh), markers of intestinal paracellular and transcellular pathways, respectively (25, 26). IP was ranging between 0.001 and 0.394 with an average of 0.07±0.007 (mean±s.e.) and is not significantly different among postnatal day 7-10 (**Supplemental Fig. 1A**). High IP was

defined by a La/Rh ratio >0.05, as validated and applied previously (16). Of the 113 subjects, 48 (42.5%) were found to have high IP. Infants <28 weeks GA were more likely to have elevated IP (N=18) than infants 28^0-32^6 weeks GA [(64.3% vs. 35.3%), P<0.01].

Postmenstrual age and mother's own breastmilk (MOM) feeding are associated with intestinal permeability in early preterm neonates. Among the collected demographic and maternal variables for each infant, four host factors were observed to be inversely related to IP, including: GA, postmenstrual age (PMA) corresponding to chronological and GA, birthweight, and 1-minute Apgar score (**Table 1**). These variables are also highly correlated to one another with high covariates multicollinearity (variance inflation factor > 10) (**Fig. S1**). PMA was the most significant factor associated with IP among the four (P = 0.01, q value = 0.015) based on Hilbert-Schmidt Independence Criterion (HSIC) (**Table S2**). Other host factors such as sex and race were not significantly associated with IP. Maternal factors including preterm premature rupture of membranes (PPROM), maternal antibiotics, antenatal corticosteroids, preeclampsia and delivery mode, were not associated with IP. These data indicate that younger infants have significantly higher incidences of high IP, likely attributed to their more immature intestinal development.

However, host factors could only partially explain IP. Mother's own breastmilk (MOM) longer feeding and higher intake volume, and shorter antibiotics treatment duration were also significantly associated with low IP (**Table 1**). Compared to infants with low IP, neonates with high IP had fewer days of MOM feeding (4 days vs. 5.5 days, P<0.01) and less total MOM volume (123.4 ml/kg vs. 263 ml/kg, P<0.01) as well as longer

duration (>3 days) antibiotics use (37.5% vs. 18.5%, P=0.03). We adjusted host factors associated with IP and fit a generalized logistic regression model. Newborns who were fed MOM for ≥4 days during the first week were demonstrated to be 10.3-fold more likely to have low IP than those who were fed MOM for <4 days [adjusted odds ratio (aOR): 10.3, 95% CI: 3.21-33.33] (**Table 2**). Additionally, newborns who had longer antibiotics treatment (≥3 days) were 2.6 times more likely to have high IP, however this association was mitigated when adjusting for confounders like PMA. This result is in line with our previous observations that antibiotic use is significantly more common in the early GA subjects (92% in <28 weeks GA *versus* 32% in >28 weeks GA, P<0.001) (16). Statistical dependence analyses showed that the cumulative intake volume of MOM prior to the IP measurement was the most significant factor associated with IP (P <0.001, q value <0.01, HSIC statistic=1.53 and 1.46), at a significance level even higher than host factors including GA (P <0.001, q value <0.01, HSIC statistics=1.12), PMA (P = 0.01, q value = 0.015, HSIC statistics=0.93), and body weight (P = 0.01, q value = 0.035, HSIC statistics=1.12) (**Table S2**).

Breastmilk intake is associated with improved intestinal barrier integrity. Unfortunately, mothers who deliver preterm often produce less milk than those who deliver term, and milk administration is often delayed especially in early preterm infants (27). Formula and/or pasteurized donor human breastmilk (PDHM) is often a necessary dietary supplement. Only 55.7% of neonates in the cohort were exclusively breastfed (N=63), others had either complemented with formula (N=31), or PDHM (N=12), or were fed exclusively formula (N=9) (**Fig. 2A**). For this reason, we investigated IP in neonates grouped by feeding types. Exclusive formula feeding was significantly associate with

high IP, either in number of days (P=0.02) or the intake volume (P=0.03, **Table 1**). However, when formula was used in combination with MOM, even at a minor portion (35.2%±31.7%, mean±s.e.), IP was significantly lowered to a level that is no different than exclusive MOM (**Fig. 2B**). Infants whose diet was supplemented with PDHM in addition to MOM had similar IP to the exclusive MOM group. We further investigated how much MOM is "sufficient" relating to improved IP during the first week post-birth. A highly elevated IP was observed in infants who received no MOM (exclusive formula or no feed), and a rapid decrease in IP was inversely correlated with increased MOM intake volume (**Fig. 2C**). Discriminatory machine learning schemes suggested that a threshold around 150-180 ml/kg of cumulative intake of MOM by 7-10 days of age is associated with low IP. Together our results indicate that sufficient MOM, used alone or combined with other forms of feeding, significantly impacts IP in early preterm infants. Even more importantly, these results imply that the benefits of breastmilk feeding are beyond the nutrition alone but extend to postnatal intestinal barrier maturation.

Increased *Bifidobacterium* species abundance correlates with improved intestinal barrier integrity. We further performed high-resolution characterization of intestinal microbiota in 517 fecal samples, using both short-read sequencing of the V3V4 region of the 16S rRNA gene on an Illumina HiSeq 2500 instrument (300PE, N=472), and long-read sequencing of the full-length 16S rRNA gene on PacBio Sequel II platform (N=192). For short-read sequencing, we obtained a total of 25,838,078 high-quality, non-chimeric ASVs (Amplicon Sequence Variants) after the assembly of forward and reverse reads and quality assessment, representing 51,165±620 (mean±s.e.) ASVs per sample (**Table B** at https://doi.org/10.6084/m9.figshare.19723252.v1). On the

other hand, long-read sequencing generated using the Circular Consensus Sequences (CCS) yielded 1,271,873 high-quality full-length 16S rRNA sequences or 992.9±16.8 (mean±s.e.) non-chimeric ASVs per sample. The full-length 16S rRNA gene sequences (1,462 bp on average) extended the partial V3V4 region (428 bp on average) 3.2 times, and afforded species level assignment for 87.6% of the long-read ASVs (remaining were not assigned due to a lack of reference), compared to 15.3% for the short-read ones (**Table D** at https://doi.org/10.6084/m9.figshare.19723252.v1**, Fig. S2**). Using samples sequenced by both methods, taxonomic assignments for long-read ASVs were conveyed to short-read ASVs using perfect sequence match, thus achieving species assignment in 65.3% of short-read sequences (**Table E** at https://doi.org/10.6084/m9.figshare.19723252.v1).

In total 508 ASVs belonging to 212 species in 15 orders and 6 phyla were identified (**Table A-C** at https://doi.org/10.6084/m9.figshare.19723252.v1). The four most abundant taxa were *Klebsiella pneumoniae*, *Escherichia coli*, *Staphylococcus epidermidis*, and *Enterobacter* spp. These taxa were predominant (>50% relative abundance) and dictated four distinct community types (**Fig. S3**). These four taxa belong to two classes Enterobacteria (*K. pneumoniae*, *E. coli*, and *Enterobacter* spp.) and Bacilli (*S. epidermidis*) and were highly prevalent (present in 86.2-94.8% samples) in both high and low IP subjects (**Fig. 3A**). They are also known “first colonizers” of the infant gut (15, 28, 29). Five other taxa, including *Enterococcus faecalis, Clostridium perfringens, Proteus mirabilis, Bifidobacterium breve,* and *Veillonella dispar*, were found to contribute to 17.4% of all sequences and detected in 47.7-86.6% of all samples. These obligate and facultative anaerobes were considered the “succession”

209 microorganisms that succeed to the first colonizers (15, 30-32). Together these nine
210 taxa accounted for 76.0% of all sequences in this dataset. Remaining sequences were
211 from a diverse array of obligate and facultative anaerobes (**Fig. S3** cluster 5).
212 A zero-inflated negative binomial random effects model (ZINBRE) was applied to
213 investigate microbial biomarkers correlated with IP. *B. breve* was the taxa the most
214 significantly associated with low IP ($P < 0.001$) during the first 7-10 days after birth
215 (**Table S3B, Fig. 3B, S4B**). The low IP group had significantly higher levels of *B. breve*,
216 more *Bifidobacterium* overall, and more MOM. An adaptive spline logistic regression
217 model was used independently to confirm the association between *B. breve* to IP and
218 MOM (**Fig. S4C,D**). Other phylotypes associated with MOM or PMA were shown in
219 **Table S3.** The high IP-associated ASVs of *S. epidermidis*, *E. coli*, *Parabacterioides*
220 *distasonis* were associated with early PMA (**Table S3A**). *Veillonella dispar* was revealed
221 to strongly associate with later PMA ($P<0.001$) but not with IP. *S. epidermidis* and *E. coli*
222 were also associated with less MOM during the first week (**Table S3C**). *B. breve* was in
223 71.7% of samples containing *Bifidobacterium*, followed by *B. longum* (21.7%). The other
224 *Bifidobacterium* species were either rare or in very low abundance (<0.1%). Temporal
225 microbiota profiling indicated that *Bifidobacterium* species reached higher abundance
226 ~5-20%) after >3d of MOM (**Fig. 3E,** https://doi.org/10.6084/m9.figshare.19709923.v1).
227 When stratified by major feeding types, *Bifidobacterium* was mostly abundant in
228 exclusive MOM or MOM supplemented with formula (**Fig. S4A**). We plotted community
229 diversity against MOM feeding volume in function of time and observed that low IP
230 infants had significantly higher diversity microbiota and higher diversity *Bifidobacterium*
231 species, when MOM reached >150 ml/kg of cumulative intake within the first week (**Fig.**

3C-D). It is worth noting that MOM is a critical but not the only contributor to the abundance of *Bifidobacterium*. 15% of the subjects received no MOM had >1% *Bifidobacterium* and 32.5% had detected level of *Bifidobacterium* (>0.1%). Overall this result further supports the importance of achieving the critical threshold of MOM intake and its critical association with low IP.

Population dynamics of *Bifidobacterium* species in early postnatal colonization. Phylogenetic analyses of full-length 16S rRNA gene sequences demonstrated that *B. breve* forms a monophyletic clade and the four most abundant ASVs were nearly identical, while *B. longum* was more phylogenetically diverse with four distinct clades (**Fig. 4A,B**). Clade I was the most abundant and represented *B. longum* subsp. *longum*, while *B. longum* in the other three clades II-IV was in low abundance. ASVs assigned to *Bifidobacterium* showed high sequence diversity (**Fig. 4A**) as well as inter- and intra-subject variability (**Fig. 4C**), in that multiple ASVs can be detected in the same subject and a single ASV can be detected in multiple subjects at multiple time points. For instance, 35 *B. longum* ASVs of four different clades were observed in one subject. Further, some ASVs (i.e., unclassified *Bifidobacterium* spp.) were only observed in infants with early PMA (<33 weeks) while others did not vary in abundance across PMA (i.e., *B. breve*), supporting a high subspecies-level diversity and population dynamics in preterm infant gut community.

To characterize the genome content of *Bifidobacterium* species, we performed whole metagenomic sequencing of 30 samples with >10% *Bifidobacterium* species using an Illumina NovaSeq 6000 platform (**Table A** at https://doi.org/10.6084/m9.figshare.19723255.v1) and generated 26 *B. breve* and four

B. longum nearly complete metagenomic-assembled genomes (MAGs) (**Table B** at https://doi.org/10.6084/m9.figshare.19723255.v1). We further performed metagenomic sequencing of two samples using Pacific Bioscience Sequel II platform, which afforded one closed and one nearly complete genomes of *B. breve* strains. The closed genome was 2.34M in size (**Fig. S6, Table C** at https://doi.org/10.6084/m9.figshare.19723255.v1), similar to the median *B. breve* genome size of 2.33M on NCBI. For pangenome analysis, we supplemented the 26 *B. breve in-house* MAGs with 107 published genomes (**Table A** at https://doi.org/10.6084/m9.figshare.19709917.v2) and the four *B. longum* MAGs with 310 published genomes (**Table B** at https://doi.org/10.6084/m9.figshare.19709917.v2) to identify homologous gene clusters (HGCs) (**Tables C-D** at https://doi.org/10.6084/m9.figshare.19709917.v2). Among the total of 4,922 *B. breve* HGCs, 54.2% were considered dispensable (present in <10% genomes), 29.4% were core (present in >95% genomes) and the rest were accessory (**Table E** at https://doi.org/10.6084/m9.figshare.19709917.v2). The pangenome of *B. longum* (7,265 HGCs) was roughly twice the size of *B. breve* (3,363 HCGs), although the two species core genomes were similar (1,511 vs. 1,448 HCGs). The large pangenome size of *B. longum* may reflect its broader host range that includes both infant and adult intestines than *B. breve* or *B. infantis,* which were exclusively observed in infant gut (33). In particular, the genes involved in the fructose 6-phosphate phosphoketolase-dependent glycolytic pathway for ATP-efficient carbohydrate catabolism, or “bifid shunt”, are conserved in both species (**Fig. S7**). Further, *B. longum*’s dispensable genome, which comprised 46.3% of its pangenome (2,666 HGCs), was smaller than that of *B.*

breve (54.2%, 3,363 HCGs) in both size and proportion, indicating a high genome plasticity in *B. breve*.

We identified 46 genes specific to *B. breve* colonizing infants with low IP (**Table F** at https://doi.org/10.6084/m9.figshare.19709917.v2). While a large number of these genes have unknown functions, others encoded functions such as glycosyl transferases, glycosyl hydrolases, cell surface adhesion and transport, polysaccharide biosynthesis, quorum sensing, and phage integration. Further, a number of functions were significantly enriched in these genomes compared to the species' genomes publicly available (adjusted q-value < 0.05, **Table F-I** at https://doi.org/10.6084/m9.figshare.19709917.v2), such as cation transmembrane transporter activity, glucuronate isomerase, methyladenine glycosylase, glycosyl hydrolase family 59, 2, 85, 30, bacterial rhamnosidase A and B. Of note, *B. breve* HGC profiles appears to be highly similar within subjects, indicating that *B. breve* genomes detected at different time points in the same infants shared greater similarity than those from different subjects (**Fig. S7**, **Table J** at https://doi.org/10.6084/m9.figshare.19709917.v2). Together, compared to *B. longum, B. breve* colonizing infants with low IP has a high genome plasticity and enriched genetic features in carbohydrate metabolism and transportation that underlies the species strong niche adaptive capabilities.

Specialized human milk oligosaccharides assimilation capabilities of Bifidobacterium strains in early preterm infants. As both *Bifidobacterium* species abundance and MOM were associated with postnatal intestinal barrier maturation, we next investigated whether these two factors were linked through the ability of

Bifidobacterium species to utilize the oligosaccharides present in breastmilk. Previously characterized major HMO utilizers like *Bacteroides* species and *Lactobacillus* (34, 35) were largely absent from our cohort (https://doi.org/10.6084/m9.figshare.19723252.v1), indicating that *Bifidobacterium* species likely provide the genetic capabilities to metabolize HMOs. We thus examined the set of genes encoding extracellular hydrolases, sugar transporters, and intracellular hydrolases (**Table S4**), which comprise the machinery necessary to uptake and metabolize HMO substrates to feed the central fermentative metabolism (36-38).

Intracellular HMO utilization functions were exclusively found encoded by both *B. breve* and *B. longum*. We examined eight essential extracellular enzymes and their homologs (details in methods section) known to be required in extracellular breakdown of HMOs into smaller molecules that are then transported intracellularly. Interestingly, none of these extracellular enzymes were found in this cohort. We investigated five essential bacterial ABC transporters and homologs involved in the import of various oligosaccharides, known to have a high specificity for HMOs conferred by substrate-binding protein (SBPs) domains (39). Both *B. breve* and *B. longum* contained *gltA* (**Table S4A**), a gene considered crucial to the import of lacto-N-tetraose (LNT). LNT comprise the core HMO structure that is catabolized via lacto-*N*-biose (LNB) intermediates (40). Further, a family 1 solute binding proteins (F1SBP) gene cluster Blon_2177, was found in both *B. breve* and *B. longum* (**Table S4B**). This cluster was found critical in the import of non-fucosylated type 1 oligosaccharides (41). None of the *B. longum* strains but the majority *B. breve* strains of this cohort (92.4%) harbor the LNnT (lacto-N- neotetraose) transporter that is encoded by *nahS*. These findings

indicate both *B. breve* and *B. longum* could transport LNB and LNT, while *B. breve* can further metabolize LNnT.

We then evaluated the capability of consuming the transported oligosaccharides, and, compared to *B. longum,* we revealed expanded metabolic capabilities of *B. breve* of this cohort to utilize a variety of HMO molecules including fucosylated or sialylated forms, in addition to the neutral types of HMOs (*i.e.*, LNB, LNT, LNnT). 17 key glycoside hydrolases (GH) involved in essential HMO degradation and utilization were investigated (**Table S4C**). Key intracellular enzymes GH2 (β-1,4-galactosidases, LacZ2/6), GH112 (GNB/LNB phosphorylase, *lnpA*), GH20 (β-N-acetylglucosaminidase), and GH42 (β-1,3-galactosidase, *lntA*, bga42A) are highly conserved in both *B. breve* and *B. longum*. These enzymes lack transmembrane domains or signal peptide sequence and are required to degrade HMOs intracellularly (42). While almost all *B. breve* contained GH95 α-fucosidase (*afcA*, homolog to Blon_2335), GH33 α-sialidase (homolog to Blon_0646), and GH20 β-N-acetylglucosaminidase (*nahA*, homolog to Blon_0459) (**Table S4C**), only a small portion of *B. longum* (~10%) contained these enzymes. Further, *B. breve* present in these preterm infants carries gene encoding GH29 α-fucosidases more often (53.8% vs. 12.7%) than *B. breve* isolated from other sources obtained from GenBank. The presence of GH29 α-fucosidase genes underlines the capability to consume fucosylated oligosaccharides such as 2'-fucosyllactose (2'-FL) and larger fucosylated HMOs such as lacto-N-fucopentaose (38, 42). The GH29 containing *B. breve* strains in our cohort also encode GH95. In fact, GH29 and GH95 α-fucosidases are highly complementary since they target specific substrate of α-1,3/4 and α-1,2 fucosyl linkages, respectively (42), and the activation of both enzymes

enables degradation and utilization of a higher variety of HMOs. Moreover, a prominent gene cluster termed FHMO (Fucosylated Human Milk Oligosaccharide) that contains both GH29 and GH95 α-fucosidases coding genes was observed in some *B. breve* strains but is largely absent from *B. longum* (**Table S4D**). This cluster was reported to enable *B. breve* strains to preferentially consume fucosylated HMOs over neutral HMOs during early bacterial growth (42). In particular, the putative fucosyl lactose SBP (BLNG_1257) present in this cluster confers glycan binding specificity and is consistently present in *B. breve* strains of this cohort but rarely in other *B. breve* in GenBank. Overall, our results revealed an expanded, specialized HMOs assimilation capability of *B. breve* strains, conferring a competitive growth advantage in the gut of this preterm infant cohort when fed breastmilk.

Host-derived glycoproteins utilization is limited to B. breve in early preterm infants. Besides HMOs, the host-derived glycoproteins such as mucin and proteoglycan (mucus or milk) are critical carbon sources to bacteria in the infant intestinal microenvironment. Human glycoproteins are often heavily sulfated and could not be metabolized without bacterial glycosidases (43, 44). We investigated two sulfatase-encoding gene clusters essential in sulfatase metabolism *ats1* and *ats2* (45, 46), and they each encode glycosulfatases and accompanying anaerobic sulfatase-maturing enzymes (anSMEs) with an associated transport system and transcriptional regulator (46). The primary mucin degradation capabilities in this cohort are shown to be limited to *B. breve* strains (**Table S4F**), as the two clusters are present in 100% of *B. breve* in our cohort and ~70% of all *B. breve* genomes available. *B. longum* rarely harbor *ats1* and no strains carry *ats2*.

In addition to sulfated residues, more than half of human colonic mucin oligosaccharides also contain sialic acid residues (47). The release of sialic acid is an initial step in the sequential degradation of mucins and sialylated HMO substrates (46, 48). Hence, we investigated the two gene clusters essential for the uptake and metabolism of sialic acid, *nagA2-nagB3* cluster (Bbr_1247, Bbr_1248) and the *nan-nag* cluster (Bbr_0160-0172) (49-51). These two gene clusters are highly conserved in *B. breve* while only present in 14% of *B. longum* genomes (**Table S6E**). Our results demonstrate the capability of foraging sulfated and/or sialylated host-derived glycoprotein is attributed to *B. breve* strains in this cohort. This metabolic versatility of *B. breve* may greatly improve its fitness and facilitate its mucosa adherence, hence facilitating the colonization under nutrient- or energy-limited conditions in the preterm infant gut environment.

DISCUSSION

Early preterm neonates are a vulnerable and challenging population that often requires intensive medical care. As a result of their premature birth, these neonates often have an aberrantly permeable intestinal barrier that fail to limit bacterial translocation. Our group has previously reported positive associations between persistently elevated intestinal permeability and delayed feeding, prolonged antibiotics exposure and altered development of the intestinal microbiota, and a lack of progressive increased abundance of *Clostridiales* (15, 16). These *Clostridiales* became abundant mostly at the end of the second week post-birth, this is after the extensive barrier maturation that occurs during the first week. In this study, we determined the minimal intake of maternal breastmilk necessary to significantly lowered IP, and identified specific *Bifidobacterium* species and strains as the biomarkers associated with low IP development in preterm infants first week of life.

We posited the benefits of breastmilk extend beyond nutrition and include improved gut barrier function, and that the two factors associated with reduced IP, MOM feeding and *Bifidobacterium* strains, at least in part, are linked by the capability of the *Bifidobacterium* to metabolize human milk oligosaccharides (illustrated in **Fig. 5**). To investigate this link, we evaluated the carbohydrate metabolizing capabilities of *Bifidobacterium* strains and uncovered a complement of genes dedicated to utilizing a wide variety of HMO molecules as well as host-derived glycoproteins. These genetic features were enriched in preterm infant gut-associated *Bifidobacterium* strains compared to those isolated from other sources like dairies or adult gut. Our results are concordant with previous studies that the establishment of a bifidobacterial dominant

community was facilitated by specific gene clusters supporting HMOs metabolism, which are absent in many adult associated bifidobacterial strains (52-55). The functional characterization of the contribution of *B. breve* metabolizing MOM to low IP would be critical to its translational significance. Future studies modeling both transcriptional activities of bifidobacterial biomarkers and host responses in a longitudinal design is warranted to address the causal-effect relationships of MOM and *Bifidobacterium* on intestinal barrier maturation. Further, the production of short chain fatty acids via carbohydrate consumption by bifidobacteria, particularly acetate and butyrate, was demonstrated to correlate with their anti-inflammatory properties and promoted the defense functions of the epithelium (56-58). Together, our study supports the notion that intestinal barrier function can develop postnatally, and this process could be induced through supplementation of breastmilk substrates as well as *Bifidobacterium* strains that consume them. These elements are promising therapeutic targets to reduce NEC and other life-threatening conditions associated with intestinal hyperpermeability.

B. breve is a known dominant *Bifidobacterium* species in both preterm and term infant gut microbiota (59) and was also observed in breastmilk and vaginal microbiota (60, 61). In human, *B. breve* appears to be exclusively in these environments and is largely absent in adult gut. The factors contributing to *B. breve* persistence in infants are not well understood. Most studies were performed using the type strain *B. breve* ATCC 15700 (JCM 1192), which has limited ability to consume HMOs (62, 63). As demonstrated by us and others, strains of *B. breve* vary greatly in their capabilities to metabolize HMOs (55). The *B. breve* strains in our cohort displayed extensive enzymatic capability designed to efficiently utilize a broad range of dietary and host-

428 derived carbohydrates and thus maximizing their colonization in the infant intestinal
429 environment. In particular, we demonstrated that LNnT utilization was exclusively limited
430 to strains of *B. breve*. Growth on LNnT was shown *in vitro* to enable *B. infantis* to
431 outcompete other species such as *Bacteroides* (64). LNnT can be fermented by specific
432 strains of *Bifidobacterium* only found in infant gut (65). Digestion of neutral HMOs (*i.e.*,
433 LNT, LNnT) was actually shown to induce a significant shift in the ratio of secreted
434 acetate to lactate compared to the catabolism of the simpler carbohydrates they contain
435 (66). Further, GH29 α-fucosidase, an uncommon enzyme correlated to the ability to
436 grow on fucosylated HMOs (38), was only enriched in *B. breve* strains in this cohort.
437 The presence of key gene sets expands *B. breve* metabolic capabilities (*i.e.*, FHMO,
438 GH29, GH95), and is reminiscent to those found in *B. infantis* ATCC 15697, the model
439 strain that can also consume a broad repertoire of HMOs (41, 67). Previous clinical
440 trials administrating *B. breve* strains in early preterm infants yield contradicted results,
441 which may relate to the different strains selection. For example, Kitajima and co-authors
442 reported a *B. breve* strain BBG could colonize the immature bowel effectively with
443 significantly fewer abnormal abdominal signs and greater weight gain in VLBW infants
444 (68). However, the clinical trial of the type strain BBG-001 in very preterm infants
445 observed no evidence of benefit in terms of preventing NEC and LOS (69). These data
446 highlight the importance of strain characterization in prophylactic supplementation of live
447 biotherapeutics. Further characterization of these key genes will be necessary to
448 understand the range of oligosaccharides *B. breve* strain can transport and consume.
449 Strains collection of *B. breve* isolated from both preterm infants with rapidly lowering IP
450 and healthy term infants should be established to achieve this important goal.

The specialized HMOs and glycoprotein utilization capabilities of *B. breve*, particularly the sulfated and sialic residues degradation, further confers a competitive capability that improve *B. breve* fitness and facilitate its adherence and colonization of the gut mucosa (70). The release of sialic acid is an initial step in the sequential degradation of mucins and sialylated HMO substrates (46, 48), and the ability to utilize the heavily sulfated mucin glycoprotein and sialic residues were found to be highly correlated (46, 49). Sialic acid concentrations are highest in colostrum in preterm infants but decrease by almost 80% after 3 months (71). Further, breastmilk from mom who delivered preterm was reported to be a rich source of oligosaccharide-bound sialic acids, with 20% more sialic acid residues than breastmilk from term mothers and 25% more than that found in formula (72). A recent *in vivo* study showed that sialylated HMOs are on the causal pathway of a microbiota-dependent infant growth outcome, hence were considered the most growth-discriminatory HMO structures (73). Interestingly, and supporting its importance in infant health, only strains of *B. infantis* and *B. breve* isolated from infant gut have been reported to be capable of utilizing sialic acid and sialylated lacto-N-tetraose as sole carbon source (54, 74, 75). A few *B. breve* strains were actually reported to preferentially consume sialylated HMOs, in particular sialyl-LNT b (LSTb), sialyl-lacto-N-hexaose (S-LNH) over neutral HMOs (38, 49). Given that bacteria with pathogenic potentials are capable of utilizing sialic acid, *B. breve* strains could rapidly sequester sialic acid away from these pathogens and offer nutritional immunity, *i.e.,* sequester nutrients to limit infection, thus contributing to a healthy intestinal environment (76). It would be highly insightful to further characterize maternal HMOs variations in MOM and the composition of specific formula in addition to the

474 information of HMOs assimilation capability of bifidobacterial strains, for comprehensive
475 understanding of the essential factors attributed to postnatal intestinal maturation.

476 HMO utilization by *Bifidobacterium* species in this cohort appears to be exclusively
477 an intracellular process, which would unlikely allow for cross-feeding of intermediates
478 with other gut bacterial species. Extracellular digestion of HMOs would afford fucose
479 and sialic acid monomers to be cross-fed to other bacteria, some of which with
480 pathogenic properties (77). *Bacteroides spp* that are largely absent in this cohort are
481 known to employ exclusively extracellular process in HMO utilization (64). The
482 “internalize, then degrade” approach for HMO consumption is a critical *Bifidobacterium*
483 property that affords protection against infection for the infants. Interestingly, the
484 preference for intracellular digestion of HMOs is not conserved across all infant gut
485 *Bifidobacterium* species or strains. A recent study revealed *Bifidobacterium* in the gut
486 microbiome of breast-fed Malawi and Venezuela infants similarly employed an
487 intracellular HMO digestion strategy, while *Bifidobacterium* in a cohort of US infants fed
488 formula and breastmilk preferentially employed extracellular HMO digestion strategies
489 (36). The difference may relate to galacto-oligosaccharides (GOS) transporter genes
490 present in strains that internalize HMOs to metabolize them, especially the GNB/LNB-
491 BP (*GltA*) gene (36, 78), though the mechanisms remain unclear.

492 Our study highlights the strong potential for the prophylactic administration of
493 specific *B. breve* strains early in life along with specific HMOs to enhance intestinal
494 barrier in preterm neonates. We previously defined a “window of opportunity” of day 8±2
495 post-birth, for intervention prior to the onset of leaky gut-associated conditions such as
496 NEC (15, 16). Our study proposed the role of breastmilk feeding in promoting the

497 growth of beneficial *Bifidobacterium* species and strains that could consume breastmilk
498 HMOs during that critical window period of time. In the absence of these prophylactic
499 *Bifidobacterium*, the benefit of breastmilk feeding is expected to be dramatically reduced.
500 Counting on the vertical transmission of these *Bifidobacterium* strains from the mothers'
501 gut or vaginal microbiota, or breastmilk is not reliable and could leave many infants
502 unprotected (79, 80). It is thus critical to gain further mechanistic insight into
503 bifidobacterial-rich microbiota formation in the infant gut by prophylactic
504 supplementation of live biotherapeutics that possess the ability to effectively utilize them.
505 Such understanding will inform the design of clinical interventions with supplementation
506 of HMOs and *Bifidobacterium* as live biotherapeutics prophylaxis to enhance intestinal
507 barrier integrity early in life, and ultimately reduce risk for NEC.

MATERIALS AND METHODS

Study cohort and feeding protocol. The study protocol was approved by the institutional review boards of the University of Maryland, Baltimore and Mercy Medical Center. Written informed parental consent was obtained. Eligibility criteria were described previously (16). 113 eligible preterm infants $24^{0/7}$-$32^{6/7}$ weeks of gestation were enrolled within 4 days after birth from combining cohorts enrolled during June 2013-October 2014 and October 2018-Nov 2019. Prior to study procedures, a complete physical exam including vital signs, weight, height, and head circumference was performed. Demographic, obstetric and clinical, medication exposures, feeding practices and adverse events data were collected from the medical record.

Enteral feeds by the orogastric or nasogastric route were initiated between the first and fourth day of life depending on clinical stability. After initial feeds of 10 ml/kg expressed breast milk or 20 kcal/oz preterm formula daily for 3-5 days, feedings were advanced by 20 ml/kg/d until 100 ml/kg/d was reached. Subsequently, caloric density was advanced to 24 kcal/oz prior to increasing feeding volume by 20 ml/kg/d to 150 ml/kg/d. The total volume of each source of feeds was calculated as sum of the daily amount of milk intake per kilogram of the administered expressed mom's breastmilk, donor milk or preterm formula from initial feed day till postnatal day 7-10 when the IP was measured. Feedings were held or discontinued for signs of feeding intolerance such as abdominal distension, gastric residuals, or hematochezia, or for clinical deterioration. Pooled pasteurized human donor breastmilk (PHDB) was purchased from Prolacta Biosciences (Duarte, CA, US). PHDB was collected from mothers of term infants who have breastfed for at least 6 months (81).

***In vivo* intestinal permeability (IP) measurement.** In our previous pilot studies that employed a small cohort of neonates (N=37) (15, 16) with IP measured at study day 1, 8±2 and 15±2. It was shown that IP is high within 4 days of birth in all preterm infants with a rapid maturation of the intestinal barrier over the first week of life. Persistently high IP and/or late increase in IP indicate the physiological immaturity of the intestinal tract barrier function. Hence the first 7-10 days in preterm infants is a critical observation period for monitoring IP. Eligible preterm infants received 1 ml/kg of the non-metabolized sugar probes on postnatal day 7-10, which included lactulose (La, Cumberland Pharmaceuticals, Nashville, TN) that is the marker of intestinal paracellular transport and rhamnose (Rh, Saccharides, Inc., Calgary, Alberta, Canada) that is the marker of intestinal transcellular transport. One ml of 8.6 g La +140 mg Rh/100 mL solution was administered enterally by nipple or by gavage via a clinically indicated orogastric tube (82). A minimum of 2 mL of urine was collected over a 4-hour period following administration of the La/Rh dose as previously described (16). La and Rh concentrations were measured by high-pressure liquid chromatography (HPLC) at the University of Calgary (Calgary, Canada). High or low intestinal permeability was defined by a La/Rh >0.05 or ≤0.05 respectively, as validated and applied previously (16). Postmenstrual age at sugar probe dosing was calculated as gestational age at birth plus postnatal age at dosing day (83).

Fecal specimen collection and nucleic acid extraction. Fecal samples (~1g) collected daily from enrollment until postnatal day 21 or NICU discharge were stored immediately in 1 ml of DNA/RNA Shield (Zymo Research, Irving, CA, USA). Stool specimen were collected from within the stool mass from the diaper as much as feasible

554 to avoid frequent air exposure. The stool sitting time was 0-3 hours and was collected
555 during diaper change every 3 hours. Urine and fecal samples were archived at -80°C
556 until processed.

557 Genomic DNA was extracted from homogenized fecal samples using the MagAttract
558 PowerMicrobiome DNA/RNA kit (Qiagen) implemented on a Hamilton STAR robotic
559 platform and after a bead-beating step on a TissueLyzer II (Qiagen) in 96-deep well
560 plates at the Microbiome Service Laboratory (MSL) at the University of Maryland
561 Baltimore (Baltimore, MD, USA). DNA purification from lysates was done on a
562 QIAsymphony automated platform.

563 **Short-read sequencing of 16S rRNA gene amplicon and whole community**
564 **metagenomes.** PCR amplification of the 16S rRNA gene V3-V4 hypervariable region
565 was performed using dual-barcoded universal primers 318F and 806R as previously
566 described (84). In brief, amplicon pools were prepared for sequencing with AMPure XT
567 beads (Beckman Coulter Genomics, Danvers, MA) and the size and quantity of the
568 amplicon library were assessed on the LabChip GX (Perkin Elmer, Waltham, MA) and
569 with the Library Quantification Kit for Illumina (Kapa Biosciences, Woburn, MA),
570 respectively. PhiX Control library (v3) (Illumina, San Diego, CA) was combined with the
571 amplicon library. High-throughput sequencing of the amplicons was performed on an
572 Illumina MiSeq platform using the 300 bp paired-end protocol. Sequence libraries were
573 prepared from the extracted DNA using the Nextera DNA Flex kit (Illumina; San Dieago,
574 CA) according to manufacturer's specifications. Libraries were then pooled together in
575 equimolar proportions and sequenced on a single Illumina NovaSeq 6000 S2 flow cell

providing an average of 6.5 million pairs of 150 bp reads per library at the Genomic Resource Center at the University of Maryland School of Medicine.

Long-read sequencing of full-length 16S rRNA gene and whole community metagenomes on Pacific Biosciences Sequel II platform. Amplification of full-length 16S rRNA gene was performed using a dual-barcode, two-step PCR on diluted (1:10) genomic DNA. The first round of PCR amplification of the 16S rRNA full-length gene was performed using universal primers 27F (AGRGTTYGATYMTGGCTCAG) and 1492R (RGYTACCTTGTTACGACTT) following Pacific Biosciences (Menlo Park, CA, USA) specifications for 20 cycles. The cycling conditions for the first-step PCR were 95C for 30sec, 57C for 30sec, and 72C for 60sec. The PCR reaction was then diluted in water (1:5) and amplified with Pacific Biosciences universal forward/reverse 96-plate primers for an additional 20 cycles following Pacific Biosciences specifications. Cycling conditions are as described in manufacture protocol (85). DNA quantification was carried out using the Quant-iT PicoGreen double-stranded DNA assay (Invitrogen) and visualized on a 2% agarose E-gel. The amplicon libraries were normalized and cleaned and concentrated using AmPure XP SPRI beads (Beckman Coulter, Brea, CA, USA) at 0.6X the reaction volume.

Library pools were prepared with SMRTBell Template Prep Kit 1.0 with barcoded adaptors. Libraries were then size-selected on a BluePippen (Sage Science, Beverly, MA) with a cutoff of 5 kb. Sequencing was performed on the Sequel II Platform (PacBio, Menlo Park, CA) with a loading at 60pM. Multiplexed samples were sequenced on PacBio Sequel II cells using the S/P3-C1/5.0-8M sequencing chemistry. Demultiplexing was done with *lima* (version 1.9.0) using default parameters except minimum barcode

score 26 and min length 50 bp, both tools are part of the SMRTLink 6.0.1 software package with updated CCS version 3.4.1 (Pacific Biosciences, 2019). Raw reads were assembled via Canu v1.8 and the "-pacbio-raw" protocol (86). Resulting contigs were taxonomically annotated using BLASTN v 2.8.1 (87) and the non-redundant nucleotide database (updated 2019/05/03) to pool all contigs identified under the same species name to form metagenomic bins. Binned contigs were circularized and rotated using "Simple-circularise" (88) and retained if the circularized contigs is in the range of the full genome size according to published closed genomes of that species based on genBank genome database. Metagenome bins were further confirmed using GTDB-Tk v1.1.0 (89). Genomes were annotated using PROKKA v1.13 (90).

Epidemiological analyses. Covariates identified based on previous literature and biological plausibility were collected at the time of enrollment of the participants and evaluated. Categorical data were compared using Fisher's exact test and continuous data using Student's t-test. Multicollinearity between covariates was assessed using Variance Inflation Factor (VIF) and Tolerance, where covariates with VIF >10 were considered collinear. Covariates with p-value < 0.05 in the bivariate analysis were considered confounding factors and were adjusted in the multivariable analysis as random factors. Generalized logistic regression was used to determine the association between IP category and continuous variables including duration of antibiotics and duration of MOM feeding. Analyses were conducted using SAS version 9.4 software (SAS Institute, Cary, NC), code used in this statistical analysis was deposited at https://github.com/igsbma/IP_microbiome/tree/main/statistical_analyses.

Bioinformatics analysis of intestinal microbiota. For 16S rRNA V3V4 gene amplicon analysis, raw data was demultiplexed and barcode, adapter and primer sequences were trimmed using tagcleaner v0.16 (91). Quality assessment and sequencing error correction was performed using the software package DADA2 v1.14 (92) and the following parameters: forward reads were truncated at position 240 and the reverse reads at position 210 based on the sequencing quality plot, no ambiguous based and a maximum of 2 expected errors per-read were allowed (93). The quality-trimmed reads were used to infer amplicon sequence variant (ASV) and their relative abundance in each sample after removing chimera. The SILVA database (94) release 132 was used to assigned taxonomy. The following criteria were applied on an ASV: 1) at least 400bp in length for long-read sequencing; 2) was observed in at least two samples; 3) at least 5 counts in at least one sample; 4) not assigned to taxonomic groups of Mitochondria or Chloroplast.

For full-length 16S rRNA gene analyses, CCS reads were generated using the ccs application with minPredictedAccuracy=0.99 and the rest of the parameters were default, including minimum 3 subread passes. Demultiplexing was done with lima (version 1.9.0) with minimum barcode score 26 and min length 50bp, both tools are part of SMRTLink 6.0.1 software package with updated CCS version 3.4.1 (Pacific Biosciences, 2019). The microbiota analyses were modified from a previously reported bioinformatics pipeline that incorporates the DADA2 protocol (95). The quality-trimmed reads were used to infer ribosomal sequence variants and their relative abundance in each sample after removing chimera. Taxonomy was assigned to each ASV generated by DADA2 using both the SILVA (release 132) database and Genome Taxonomy Database (GTDB)

644 (96) and the RDP naïve Bayesian classifier as implemented in the *dada2* R package (97,
645 98). In a few cases when conflicted taxonomic assignments appeared, NCBI Refseq
646 16S rRNA combined with RDP database (99, 100) and Human Intestinal 16S rRNA
647 database (HITdb v1) (101) were used to resolve the conflict. Pacific Biosciences long-
648 reads sequencing complements short-reads sequencing for its high accuracy and
649 extended length. To boost taxonomy assignment for short sequencing, we performed
650 BLASTN search of the short-read ASVs to the long-read ASVs, and assigned the
651 taxonomic name to the short reads if there is 100% percent identity and unanimous
652 assignment if there are multiple hits to long-reads sequences.
653 A heatmap was constructed from the 50 most abundant intestinal bacterial taxa
654 relative abundance in samples collected from 113 preterm infants enrolled in the study.
655 The ASVs were normalized using total sum to calculate their relative abundances. Ward
656 linkage clustering was used to cluster samples based on their Jensen-Shannon
657 distance calculated in vegan package in R (102). The number of clusters was validated
658 using gap statistics implemented in the *cluster* package in R (103) by calculating the
659 goodness of clustering measure. Package raxml (v8.0.0) (104) was used to construct
660 the phylogeny, Phyloseq R package (v1.38.0) (105) was used to display the phylogeny
661 and the barplot. Volatility plot to demonstrate the fluctuation of microbial community
662 diversity (characterized as Shannon diversity index) over MOM feeding volume in high
663 or low IP groups. Plot was generated in QIIME (2019.10 vers) (106) (option -longitudinal
664 plot-feature-volatility).
665 **Statistical analysis of intestinal microbial community.** Hilbert-Schmidt
666 Independence Criterion (HSIC) R package ‘dHSIC’ (107) was used to examine the

667 independence between any variables with IP. Longitudinal modeling was performed
668 using zero-inflated negative binomial random effects (ZINBRE) models. These models
669 account for the possibility of existence of more than expected zeros (from negative
670 binomial distribution) as well for correlations between samples from the same subject.
671 Though IP was categorized to high and low groups, it is inherently continuous and
672 hence we modeled IP as continuous value in our analyses. Subject was included as a
673 random factor. Read counts data of phylotypes detected in at least 15% samples were
674 modeled using ZINBRE models. The same principle was applied to MOM and PMA.
675 The model was fitted using JAGS R package (108), and 10,000 iterations with the same
676 number of burn in iterations was used. The convergence of the model was assessed
677 using Gelman and Rubin's potential scale reduction factor (109) and visual inspection of
678 each coefficient's Markov chains. The mean of the posterior distributions of estimated
679 coefficients and their corresponding 95% credible intervals were calculated using
680 model's Markov chains. The credible intervals without overlapping are considered
681 significant. P values were computed assuming normality of the posterior distributions of
682 the corresponding coefficients. An adaptive spline logistic regression model
683 implemented in spmrf R package (110) was used independently to confirm the
684 association between B. breve to IP and MOM. This model is a locally adaptive
685 nonparametric fitting method that operates within a Bayesian framework, which uses
686 shrinkage prior Markov random fields to induce sparsity and provides a combination of
687 local adaptation and global control (110). Bayesian goodness-of-fit p-value implemented
688 in R package rstan (111) was used to access the significance of the association. R code
689 implementation of the model is deposited in

https://github.com/igsbma/IP_microbiome/tree/main/statistical_analyses. Discriminatory machine learning schemes computation were implemented in weka (112, 113), including J48 decision tree, REPTree, decision stump, and logistic model trees. The functional enrichment test was performed for each functional group (based on COG and PFAM annotation) and each of homologous gene cluster (HGC) generated in genome comparison analyses. The frequency tables of each function or HGC in each category (*i.e.*, MAGs of this study versus genBank genomes) were generated, which was used to fit a generalized linear model with the logit linkage function to compute an enrichment score and p-value for each unit (114). False detection rate correction to p-values was used to account for multiple tests using R package 'qvalue' (115).

Intestinal microbiome analyses. Metagenomic sequence data were pre-processed using the following steps: 1) human sequence reads and rRNA LSU/SSU reads were removed using BMTagger v3.101 (116) using a standard human genome reference (GRCh37.p5) (117); 2) rRNA sequence reads were removed *in silico* by aligning all reads using Bowtie v1 (118) to the SILVA PARC ribosomal-subunit sequence database (94). Sequence read pairs were removed even if only one of the reads matched to the human genome reference or to rRNA; 3) the Illumina adapter was trimmed using Trimmomatic (119); 4) sequence reads with average quality greater than Q15 over a sliding window of 4 bp were trimmed before the window, assessed for length and removed if less than 75% of the original length; and 5) no ambiguous base pairs were allowed. The taxonomic composition of the microbiomes was established using MetaPhlAn version 2 (120). Metagenome assembled genomes (MAGs) pipeline includes *de bruijin* genome assembly using SPAdes v.3.10.1 (121), the bins were

713 defined through distance clustering based on coverage and tetranucleotide signature
714 using MetaBat v2 (122), and were refined using GTDB-Tk (89). Genomes were
715 annotated using PROKKA v1.13 (90), annotated through evidences from the
716 nomenclature of the consortium for function glycomics, eggNOG (v4.5)(123), KEGG
717 2013-03-18 release (124)), Pfam (v30.0)(125), CAZy (2014 release) (126, 127).
718 Similarity searches were performed to compare with previously annotated enzymes or
719 transporter proteins based on the accession number (36-38), using BLASTP and
720 confirmed with the COG, Pfam and CAZy annotation evidence to ensure the integrity of
721 the results. The 8 essential extracellular enzymes that are known to be required in
722 extracellular cleavage of HMOs before importing selected products of degradation are
723 investigated (36-38), include: 1,2-α-l-Fucosidase (AfcA), 1,3/4-α-l-Fucosidase (AfcB),
724 2,3/6-α-Sialidase (SiaBb2), Lacto-N-biosidase (LnbB, LnbX), Chaperon for LnbX (LnbY),
725 β-1,4-Galactosidase (BbgIII), β-N-Acetylglucosaminidase (BbhI). Five essential bacterial
726 ABC transporters and homologs involved in the import of oligosaccharides were
727 examined, which was known to show an exquisite specificity conferred by substrate-
728 binding protein (SBPs) for different HMO molecules (39), including GNB/LNB (galacto-
729 N-biose/lacto-N-biose I) transporter SBP (GltA), FL transporter SBPs (FL1-BP, FL2-BP),
730 and LN*n*T transporter SBP (NahS). In addition to similarity search on *Bifidobacterium*
731 genomes and MAGs, we also confirmed the results by searching the metagenomic
732 community gene content, so to verify the target genes are not from species other than
733 *Bifidobacterium*.
734 Metapangenomes were prepared using the MAGs constructed in this study and
735 publicly available genomes under the species name *B. breve* (taxID: 1685) and *B.*

longum (taxID: 216816), listed in **Table S6**. The metapangenome was constructed using anvi'o vers 6.2 (128) following pangenome workflow (114). Homologous gene clusters (HGCs) were identified in this set of genomes based on all-versus-all sequence similarity. Briefly, this workflow uses BLASTP to compute ANI identity between all pairs of genes, uses the Markov Cluster Algorithm (MCL) (129) to generate homologous gene clusters and aligns amino acid sequences using MUSCLE (130) for each gene cluster. Each gene was assigned to core or accessory according the hierarchical clustering of the gene clusters. Sourmash vers 3.3 (131) was used to compute ANI across genomes. To count as being present in the sample, it had to be at least 50 reads mapping on at least one *Bifidobacterium* species genomes, and the total abundance had to be at least 0.1% after normalizing over the total number of reads. For long-read data sequenced on Pacific Biosciences Sequel II platform, QC and assembly was performed using Canu-1.8 (86). The assemblies were assigned species name through BLAST to refseq dataset and confirmed with GTDB-Tk v1.1.0 (89). Genome alignment of the assemblies assigned to *B. breve* was aligned to reference *B. breve* genome JCM1192 using MAUVE aligner (132, 133).

Data and Code Availability. All metagenomicm, metataxonomic and genomic data were deposited under BioProject PRJNA774819 (https://www.ncbi.nlm.nih.gov/bioproject/PRJNA774819) for open assessment. Illumina 16S rRNA V3V4 gene amplicon and Pacific Biosciences full-length 16S rRNA gene data were deposited in Sequence Read Archive with experiment ID from SRX12805867 to SRX12806634. Data deposition includes samples of positive and negative controls in each plate. Metagenomic data using Pacific Biosciences were deposited in

SRR16598000 and SRR16598001. Metagenomic data using Illumina platform were deposited in the same BioProject with experiment ID from SRX12798907 to SRX12798933. The assembled genomes of *B breve* were deposited under the accession ID JAJGBR000000000 and JAJGBS000000000. The R code processing these sequences and SAS code used in this statistical analysis are deposited in https://github.com/igsbma/IP_microbiome/tree/main/statistical_analyses. Detailed information of sequences and annotation of pangenome can be retrieved at https://github.com/igsbma/IP_microbiome/tree/main/pangenome.

SUPPLEMENTAL MATERIALS

FIGURE S1, PDF file
FIGURE S2, PDF file
FIGURE S3, PDF file
FIGURE S4, PDF file
FIGURE S5, PDF file
FIGURE S6, PDF file
TABLE S1, Excel file
TABLE S2, Word file
TABLE S3, Excel file
TABLE S4, Excel file

CONTRIBUTIONS

B.M., J.R., S.S., and R.V. designed the research; S.S., E.J., E.M., B.M., G.N., H.Y., L.S.R. and R.V. conducted the clinical study; B.M., H.Y., L.F., and M.H. conducted the short-read sequencing; B.M., E.M., M.H., L.S., L.J.T. conducted the long-read sequencing; B.M., M.F, and P.G. performed the statistical analyses; B.M. and G.N.

784 performed the epidemiological analyses; B.M., S.S., J.M.L-D., G.N., M.F., M.F.P., J.R.,
785 and R.V. wrote the paper.

786 ACKNOWLEDGEMENTS

787 This study was supported in part by The Gerber Foundation 2018 award (Project ID
788 6361), the National Institute of Diabetes and Digestive and Kidney Diseases (NIDDK) of
789 the National Institute of health under award number R21DK123674, and the Institute for
790 Clinical and Translational Research (ICTR) at University of Maryland Accelerated
791 Translational Incubator Pilot (ATIP) award. The authors thank Dr. Jonathan Meddings
792 and Mr. Kim Le at the University of Calgary, Calgary, Alberta, Canada for the HPLC
793 analysis of serum and urine samples. Ms. Ivette Santana-Cruz (GRC at IGS) for
794 constructive discussion on long-read data processing. Ms. Shilpa Narina and Sarah
795 Arbaugh for great assistance in clinical specimen collection.

REFERENCES

1. Hunter CJ, Upperman JS, Ford HR, Camerini V. 2008. Understanding the susceptibility of the premature infant to necrotizing enterocolitis (NEC). Pediatr Res 63:117-23.
2. Fitzgibbons SC, Ching Y, Yu D, Carpenter J, Kenny M, Weldon C, Lillehei C, Valim C, Horbar JD, Jaksic T. 2009. Mortality of necrotizing enterocolitis expressed by birth weight categories. J Pediatr Surg 44:1072-5; discussion 1075-6.
3. Fox TP, Godavitarne C. 2012. What really causes necrotising enterocolitis? ISRN Gastroenterol 2012:628317.
4. Anand RJ, Leaphart CL, Mollen KP, Hackam DJ. 2007. The role of the intestinal barrier in the pathogenesis of necrotizing enterocolitis. Shock 27:124-33.
5. Bergmann KR, Liu SX, Tian R, Kushnir A, Turner JR, Li HL, Chou PM, Weber CR, De Plaen IG. 2013. Bifidobacteria stabilize claudins at tight junctions and prevent intestinal barrier dysfunction in mouse necrotizing enterocolitis. Am J Pathol 182:1595-606.
6. Fasano A. 2008. Physiological, pathological, and therapeutic implications of zonulin-mediated intestinal barrier modulation: living life on the edge of the wall. Am J Pathol 173:1243-52.
7. Nanthakumar N, Meng D, Goldstein AM, Zhu W, Lu L, Uauy R, Llanos A, Claud EC, Walker WA. 2011. The mechanism of excessive intestinal inflammation in necrotizing enterocolitis: an immature innate immune response. PLoS One 6:e17776.
8. Claud EC, Walker WA. 2008. Bacterial colonization, probiotics, and necrotizing enterocolitis. J Clin Gastroenterol 42 Suppl 2:S46-52.
9. Berman L, Moss RL. 2011. Necrotizing enterocolitis: an update. Semin Fetal Neonatal Med 16:145-50.
10. Guner YS, Friedlich P, Wee CP, Dorey F, Camerini V, Upperman JS. 2009. State-based analysis of necrotizing enterocolitis outcomes. J Surg Res 157:21-9.
11. Ganapathy V, Hay JW, Kim JH. 2012. Costs of necrotizing enterocolitis and cost-effectiveness of exclusively human milk-based products in feeding extremely premature infants. Breastfeed Med 7:29-37.
12. Neu J, Walker WA. 2011. Necrotizing enterocolitis. N Engl J Med 364:255-64.
13. Claud EC. 2009. Neonatal Necrotizing Enterocolitis -Inflammation and Intestinal Immaturity. Antiinflamm Antiallergy Agents Med Chem 8:248-259.
14. Neish AS. 2009. Microbes in gastrointestinal health and disease. Gastroenterology 136:65-80.
15. Ma B, McComb E, Gajer P, Yang H, Humphrys M, Okogbule-Wonodi AC, Fasano A, Ravel J, Viscardi RM. 2018. Microbial Biomarkers of Intestinal Barrier Maturation in Preterm Infants. Front Microbiol 9:2755.
16. Saleem B, Okogbule-Wonodi AC, Fasano A, Magder LS, Ravel J, Kapoor S, Viscardi RM. 2017. Intestinal Barrier Maturation in Very Low Birthweight Infants: Relationship to Feeding and Antibiotic Exposure. J Pediatr 183:31-36 e1.
17. Weaver LT, Laker MF, Nelson R. 1984. Intestinal permeability in the newborn. Arch Dis Child 59:236-41.
18. Halpern MD, Denning PW. 2015. The role of intestinal epithelial barrier function in the development of NEC. Tissue Barriers 3:e1000707.

19. Walker AW, Martin JC, Scott P, Parkhill J, Flint HJ, Scott KP. 2015. 16S rRNA gene-based profiling of the human infant gut microbiota is strongly influenced by sample processing and PCR primer choice. Microbiome 3:26.
20. Frank JA, Reich CI, Sharma S, Weisbaum JS, Wilson BA, Olsen GJ. 2008. Critical evaluation of two primers commonly used for amplification of bacterial 16S rRNA genes. Appl Environ Microbiol 74:2461-70.
21. Sim K, Cox MJ, Wopereis H, Martin R, Knol J, Li MS, Cookson WO, Moffatt MF, Kroll JS. 2012. Improved detection of bifidobacteria with optimised 16S rRNA-gene based pyrosequencing. PLoS One 7:e32543.
22. Stewart CJ, Ajami NJ, O'Brien JL, Hutchinson DS, Smith DP, Wong MC, Ross MC, Lloyd RE, Doddapaneni H, Metcalf GA, Muzny D, Gibbs RA, Vatanen T, Huttenhower C, Xavier RJ, Rewers M, Hagopian W, Toppari J, Ziegler AG, She JX, Akolkar B, Lernmark A, Hyoty H, Vehik K, Krischer JP, Petrosino JF. 2018. Temporal development of the gut microbiome in early childhood from the TEDDY study. Nature 562:583-588.
23. O'Connell Motherway M, Houston A, O'Callaghan G, Reunanen J, O'Brien F, O'Driscoll T, Casey PG, de Vos WM, van Sinderen D, Shanahan F. 2019. A Bifidobacterial pilus-associated protein promotes colonic epithelial proliferation. Mol Microbiol 111:287-301.
24. Sonnenburg JL, Chen CT, Gordon JI. 2006. Genomic and metabolic studies of the impact of probiotics on a model gut symbiont and host. PLoS Biol 4:e413.
25. van Wijck K, Bessems BA, van Eijk HM, Buurman WA, Dejong CH, Lenaerts K. 2012. Polyethylene glycol versus dual sugar assay for gastrointestinal permeability analysis: is it time to choose? Clin Exp Gastroenterol 5:139-50.
26. van Wijck K, Verlinden TJ, van Eijk HM, Dekker J, Buurman WA, Dejong CH, Lenaerts K. 2013. Novel multi-sugar assay for site-specific gastrointestinal permeability analysis: a randomized controlled crossover trial. Clin Nutr 32:245-51.
27. Asztalos EV. 2018. Supporting Mothers of Very Preterm Infants and Breast Milk Production: A Review of the Role of Galactogogues. Nutrients 10.
28. Bittinger K, Zhao C, Li Y, Ford E, Friedman ES, Ni J, Kulkarni CV, Cai J, Tian Y, Liu Q, Patterson AD, Sarkar D, Chan SHJ, Maranas C, Saha-Shah A, Lund P, Garcia BA, Mattei LM, Gerber JS, Elovitz MA, Kelly A, DeRusso P, Kim D, Hofstaedter CE, Goulian M, Li H, Bushman FD, Zemel BS, Wu GD. 2020. Bacterial colonization reprograms the neonatal gut metabolome. Nat Microbiol 5:838-847.
29. Del Chierico F, Vernocchi P, Petrucca A, Paci P, Fuentes S, Pratico G, Capuani G, Masotti A, Reddel S, Russo A, Vallone C, Salvatori G, Buffone E, Signore F, Rigon G, Dotta A, Miccheli A, de Vos WM, Dallapiccola B, Putignani L. 2015. Phylogenetic and Metabolic Tracking of Gut Microbiota during Perinatal Development. PLoS One 10:e0137347.
30. La Rosa PS, Warner BB, Zhou Y, Weinstock GM, Sodergren E, Hall-Moore CM, Stevens HJ, Bennett WE, Jr., Shaikh N, Linneman LA, Hoffmann JA, Hamvas A, Deych E, Shands BA, Shannon WD, Tarr PI. 2014. Patterned progression of bacterial populations in the premature infant gut. Proc Natl Acad Sci U S A 111:12522-7.
31. Backhed F, Roswall J, Peng Y, Feng Q, Jia H, Kovatcheva-Datchary P, Li Y, Xia Y, Xie H, Zhong H, Khan MT, Zhang J, Li J, Xiao L, Al-Aama J, Zhang D, Lee YS, Kotowska D, Colding C, Tremaroli V, Yin Y, Bergman S, Xu X, Madsen L, Kristiansen K, Dahlgren J, Wang J. 2015.

882 Dynamics and Stabilization of the Human Gut Microbiome during the First Year of Life.
883 Cell Host Microbe 17:690-703.
884 32. Robertson RC, Manges AR, Finlay BB, Prendergast AJ. 2019. The Human Microbiome and
885 Child Growth - First 1000 Days and Beyond. Trends Microbiol 27:131-147.
886 33. Odamaki T, Bottacini F, Kato K, Mitsuyama E, Yoshida K, Horigome A, Xiao JZ, van
887 Sinderen D. 2018. Genomic diversity and distribution of Bifidobacterium longum subsp.
888 longum across the human lifespan. Sci Rep 8:85.
889 34. Zuniga M, Monedero V, Yebra MJ. 2018. Utilization of Host-Derived Glycans by Intestinal
890 Lactobacillus and Bifidobacterium Species. Front Microbiol 9:1917.
891 35. Martens EC, Chiang HC, Gordon JI. 2008. Mucosal glycan foraging enhances fitness and
892 transmission of a saccharolytic human gut bacterial symbiont. Cell Host Microbe 4:447-
893 57.
894 36. Sakanaka M, Gotoh A, Yoshida K, Odamaki T, Koguchi H, Xiao JZ, Kitaoka M, Katayama T.
895 2019. Varied Pathways of Infant Gut-Associated Bifidobacterium to Assimilate Human
896 Milk Oligosaccharides: Prevalence of the Gene Set and Its Correlation with
897 Bifidobacteria-Rich Microbiota Formation. Nutrients 12.
898 37. Odamaki T, Horigome A, Sugahara H, Hashikura N, Minami J, Xiao JZ, Abe F. 2015.
899 Comparative Genomics Revealed Genetic Diversity and Species/Strain-Level Differences
900 in Carbohydrate Metabolism of Three Probiotic Bifidobacterial Species. Int J Genomics
901 2015:567809.
902 38. Ruiz-Moyano S, Totten SM, Garrido DA, Smilowitz JT, German JB, Lebrilla CB, Mills DA.
903 2013. Variation in consumption of human milk oligosaccharides by infant gut-associated
904 strains of Bifidobacterium breve. Appl Environ Microbiol 79:6040-9.
905 39. Tam R, Saier MH, Jr. 1993. Structural, functional, and evolutionary relationships among
906 extracellular solute-binding receptors of bacteria. Microbiol Rev 57:320-46.
907 40. Suzuki R, Wada J, Katayama T, Fushinobu S, Wakagi T, Shoun H, Sugimoto H, Tanaka A,
908 Kumagai H, Ashida H, Kitaoka M, Yamamoto K. 2008. Structural and thermodynamic
909 analyses of solute-binding Protein from Bifidobacterium longum specific for core 1
910 disaccharide and lacto-N-biose I. J Biol Chem 283:13165-73.
911 41. Garrido D, Kim JH, German JB, Raybould HE, Mills DA. 2011. Oligosaccharide binding
912 proteins from Bifidobacterium longum subsp. infantis reveal a preference for host
913 glycans. PLoS One 6:e17315.
914 42. Garrido D, Ruiz-Moyano S, Kirmiz N, Davis JC, Totten SM, Lemay DG, Ugalde JA, German
915 JB, Lebrilla CB, Mills DA. 2016. A novel gene cluster allows preferential utilization of
916 fucosylated milk oligosaccharides in Bifidobacterium longum subsp. longum SC596. Sci
917 Rep 6:35045.
918 43. Robertson AM, Wright DP. 1997. Bacterial glycosulphatases and sulphomucin
919 degradation. Can J Gastroenterol 11:361-6.
920 44. Filipe MI. 1979. Mucins in the human gastrointestinal epithelium: a review. Invest Cell
921 Pathol 2:195-216.
922 45. Berteau O, Guillot A, Benjdia A, Rabot S. 2006. A new type of bacterial sulfatase reveals
923 a novel maturation pathway in prokaryotes. J Biol Chem 281:22464-70.

924 46. Egan M, Jiang H, O'Connell Motherway M, Oscarson S, van Sinderen D. 2016.
925 Glycosulfatase-Encoding Gene Cluster in Bifidobacterium breve UCC2003. Appl Environ
926 Microbiol 82:6611-6623.
927 47. Corfield AP, Wagner SA, Safe A, Mountford RA, Clamp JR, Kamerling JP, Vliegenthart JF,
928 Schauer R. 1993. Sialic acids in human gastric aspirates: detection of 9-O-lactyl- and 9-O-
929 acetyl-N-acetylneuraminic acids and a decrease in total sialic acid concentration with
930 age. Clin Sci (Lond) 84:573-9.
931 48. Robbe C, Capon C, Maes E, Rousset M, Zweibaum A, Zanetta JP, Michalski JC. 2003.
932 Evidence of regio-specific glycosylation in human intestinal mucins: presence of an
933 acidic gradient along the intestinal tract. J Biol Chem 278:46337-48.
934 49. Egan M, O'Connell Motherway M, Ventura M, van Sinderen D. 2014. Metabolism of
935 sialic acid by Bifidobacterium breve UCC2003. Appl Environ Microbiol 80:4414-26.
936 50. Podolsky DK. 1985. Oligosaccharide structures of human colonic mucin. J Biol Chem
937 260:8262-71.
938 51. Kunz C, Rudloff S, Baier W, Klein N, Strobel S. 2000. Oligosaccharides in human milk:
939 structural, functional, and metabolic aspects. Annu Rev Nutr 20:699-722.
940 52. Turroni F, Milani C, Duranti S, Mahony J, van Sinderen D, Ventura M. 2018. Glycan
941 Utilization and Cross-Feeding Activities by Bifidobacteria. Trends Microbiol 26:339-350.
942 53. Ferretti P, Pasolli E, Tett A, Asnicar F, Gorfer V, Fedi S, Armanini F, Truong DT, Manara S,
943 Zolfo M, Beghini F, Bertorelli R, De Sanctis V, Bariletti I, Canto R, Clementi R, Cologna M,
944 Crifo T, Cusumano G, Gottardi S, Innamorati C, Mase C, Postai D, Savoi D, Duranti S, Lugli
945 GA, Mancabelli L, Turroni F, Ferrario C, Milani C, Mangifesta M, Anzalone R, Viappiani A,
946 Yassour M, Vlamakis H, Xavier R, Collado CM, Koren O, Tateo S, Soffiati M, Pedrotti A,
947 Ventura M, Huttenhower C, Bork P, Segata N. 2018. Mother-to-Infant Microbial
948 Transmission from Different Body Sites Shapes the Developing Infant Gut Microbiome.
949 Cell Host Microbe 24:133-145 e5.
950 54. Sela DA, Chapman J, Adeuya A, Kim JH, Chen F, Whitehead TR, Lapidus A, Rokhsar DS,
951 Lebrilla CB, German JB, Price NP, Richardson PM, Mills DA. 2008. The genome sequence
952 of Bifidobacterium longum subsp. infantis reveals adaptations for milk utilization within
953 the infant microbiome. Proc Natl Acad Sci U S A 105:18964-9.
954 55. James K, Motherway MO, Bottacini F, van Sinderen D. 2016. Bifidobacterium breve
955 UCC2003 metabolises the human milk oligosaccharides lacto-N-tetraose and lacto-N-
956 neo-tetraose through overlapping, yet distinct pathways. Sci Rep 6:38560.
957 56. Fukuda S, Toh H, Hase K, Oshima K, Nakanishi Y, Yoshimura K, Tobe T, Clarke JM,
958 Topping DL, Suzuki T, Taylor TD, Itoh K, Kikuchi J, Morita H, Hattori M, Ohno H. 2011.
959 Bifidobacteria can protect from enteropathogenic infection through production of
960 acetate. Nature 469:543-7.
961 57. Alcon-Giner C, Dalby MJ, Caim S, Ketskemety J, Shaw A, Sim K, Lawson MAE, Kiu R,
962 Leclaire C, Chalklen L, Kujawska M, Mitra S, Fardus-Reid F, Belteki G, McColl K, Swann JR,
963 Kroll JS, Clarke P, Hall LJ. 2020. Microbiota Supplementation with Bifidobacterium and
964 Lactobacillus Modifies the Preterm Infant Gut Microbiota and Metabolome: An
965 Observational Study. Cell Rep Med 1:100077.

58. Lawson MAE, O'Neill IJ, Kujawska M, Gowrinadh Javvadi S, Wijeyesekera A, Flegg Z, Chalklen L, Hall LJ. 2020. Breast milk-derived human milk oligosaccharides promote Bifidobacterium interactions within a single ecosystem. ISME J 14:635-648.
59. Turroni F, Peano C, Pass DA, Foroni E, Severgnini M, Claesson MJ, Kerr C, Hourihane J, Murray D, Fuligni F, Gueimonde M, Margolles A, De Bellis G, O'Toole PW, van Sinderen D, Marchesi JR, Ventura M. 2012. Diversity of bifidobacteria within the infant gut microbiota. PLoS One 7:e36957.
60. Soto A, Martin V, Jimenez E, Mader I, Rodriguez JM, Fernandez L. 2014. Lactobacilli and bifidobacteria in human breast milk: influence of antibiotherapy and other host and clinical factors. J Pediatr Gastroenterol Nutr 59:78-88.
61. Ma B, France MT, Crabtree J, Holm JB, Humphrys MS, Brotman RM, Ravel J. 2020. A comprehensive non-redundant gene catalog reveals extensive within-community intraspecies diversity in the human vagina. Nat Commun 11:940.
62. LoCascio RG, Ninonuevo MR, Freeman SL, Sela DA, Grimm R, Lebrilla CB, Mills DA, German JB. 2007. Glycoprofiling of bifidobacterial consumption of human milk oligosaccharides demonstrates strain specific, preferential consumption of small chain glycans secreted in early human lactation. J Agric Food Chem 55:8914-9.
63. Strum JS, Kim J, Wu S, De Leoz ML, Peacock K, Grimm R, German JB, Mills DA, Lebrilla CB. 2012. Identification and accurate quantitation of biological oligosaccharide mixtures. Anal Chem 84:7793-801.
64. Marcobal A, Barboza M, Sonnenburg ED, Pudlo N, Martens EC, Desai P, Lebrilla CB, Weimer BC, Mills DA, German JB, Sonnenburg JL. 2011. Bacteroides in the infant gut consume milk oligosaccharides via mucus-utilization pathways. Cell Host Microbe 10:507-14.
65. Miwa M, Horimoto T, Kiyohara M, Katayama T, Kitaoka M, Ashida H, Yamamoto K. 2010. Cooperation of beta-galactosidase and beta-N-acetylhexosaminidase from bifidobacteria in assimilation of human milk oligosaccharides with type 2 structure. Glycobiology 20:1402-9.
66. Ozcan E, Sela DA. 2018. Inefficient Metabolism of the Human Milk Oligosaccharides Lacto-N-tetraose and Lacto-N-neotetraose Shifts Bifidobacterium longum subsp. infantis Physiology. Front Nutr 5:46.
67. Garrido D, Dallas DC, Mills DA. 2013. Consumption of human milk glycoconjugates by infant-associated bifidobacteria: mechanisms and implications. Microbiology 159:649-664.
68. Kitajima H, Sumida Y, Tanaka R, Yuki N, Takayama H, Fujimura M. 1997. Early administration of Bifidobacterium breve to preterm infants: randomised controlled trial. Arch Dis Child Fetal Neonatal Ed 76:F101-7.
69. Costeloe K, Hardy P, Juszczak E, Wilks M, Millar MR, Probiotics in Preterm Infants Study Collaborative G. 2016. Bifidobacterium breve BBG-001 in very preterm infants: a randomised controlled phase 3 trial. Lancet 387:649-660.
70. Tailford LE, Crost EH, Kavanaugh D, Juge N. 2015. Mucin glycan foraging in the human gut microbiome. Front Genet 6:81.
71. Wang B, Brand-Miller J, McVeagh P, Petocz P. 2001. Concentration and distribution of sialic acid in human milk and infant formulas. Am J Clin Nutr 74:510-5.

72. De Leoz ML, Gaerlan SC, Strum JS, Dimapasoc LM, Mirmiran M, Tancredi DJ, Smilowitz JT, Kalanetra KM, Mills DA, German JB, Lebrilla CB, Underwood MA. 2012. Lacto-N-tetraose, fucosylation, and secretor status are highly variable in human milk oligosaccharides from women delivering preterm. J Proteome Res 11:4662-72.
73. Charbonneau MR, O'Donnell D, Blanton LV, Totten SM, Davis JC, Barratt MJ, Cheng J, Guruge J, Talcott M, Bain JR, Muehlbauer MJ, Ilkayeva O, Wu C, Struckmeyer T, Barile D, Mangani C, Jorgensen J, Fan YM, Maleta K, Dewey KG, Ashorn P, Newgard CB, Lebrilla C, Mills DA, Gordon JI. 2016. Sialylated Milk Oligosaccharides Promote Microbiota-Dependent Growth in Models of Infant Undernutrition. Cell 164:859-71.
74. Ward RE, Ninonuevo M, Mills DA, Lebrilla CB, German JB. 2007. In vitro fermentability of human milk oligosaccharides by several strains of bifidobacteria. Mol Nutr Food Res 51:1398-405.
75. Sela DA, Li Y, Lerno L, Wu S, Marcobal AM, German JB, Chen X, Lebrilla CB, Mills DA. 2011. An infant-associated bacterial commensal utilizes breast milk sialyloligosaccharides. J Biol Chem 286:11909-18.
76. Hood MI, Skaar EP. 2012. Nutritional immunity: transition metals at the pathogen-host interface. Nat Rev Microbiol 10:525-37.
77. Ng KM, Ferreyra JA, Higginbottom SK, Lynch JB, Kashyap PC, Gopinath S, Naidu N, Choudhury B, Weimer BC, Monack DM, Sonnenburg JL. 2013. Microbiota-liberated host sugars facilitate post-antibiotic expansion of enteric pathogens. Nature 502:96-9.
78. Sotoya H, Shigehisa A, Hara T, Matsumoto H, Hatano H, Matsuki T. 2017. Identification of genes involved in galactooligosaccharide utilization in Bifidobacterium breve strain YIT 4014(T). Microbiology (Reading) 163:1420-1428.
79. Cortes-Macias E, Selma-Royo M, Garcia-Mantrana I, Calatayud M, Gonzalez S, Martinez-Costa C, Collado MC. 2021. Maternal Diet Shapes the Breast Milk Microbiota Composition and Diversity: Impact of Mode of Delivery and Antibiotic Exposure. J Nutr 151:330-340.
80. Wang S, Ryan CA, Boyaval P, Dempsey EM, Ross RP, Stanton C. 2020. Maternal Vertical Transmission Affecting Early-life Microbiota Development. Trends Microbiol 28:28-45.
81. Kim J, Unger S. 2010. Human milk banking. Paediatr Child Health 15:595-602.
82. Rouwet EV, Heineman E, Buurman WA, ter Riet G, Ramsay G, Blanco CE. 2002. Intestinal permeability and carrier-mediated monosaccharide absorption in preterm neonates during the early postnatal period. Pediatr Res 51:64-70.
83. Grier A, Qiu X, Bandyopadhyay S, Holden-Wiltse J, Kessler HA, Gill AL, Hamilton B, Huyck H, Misra S, Mariani TJ, Ryan RM, Scholer L, Scheible KM, Lee YH, Caserta MT, Pryhuber GS, Gill SR. 2017. Impact of prematurity and nutrition on the developing gut microbiome and preterm infant growth. Microbiome 5:158.
84. Fadrosh DW, Ma B, Gajer P, Sengamalay N, Ott S, Brotman RM, Ravel J. 2014. An improved dual-indexing approach for multiplexed 16S rRNA gene sequencing on the Illumina MiSeq platform. Microbiome 2:6.
85. Biosciences P. 2019. Procedure & Checklist – Amplification of Full-Length 16S Gene with Barcoded Primers for Multiplexed SMRTbell® Library Preparation and Sequencing. https://www.pacb.com/wp-content/uploads/Procedure-Checklist-Full-Length-16S-Amplification-SMRTbell-Library-Preparation-an. Accessed

86. Koren S, Walenz BP, Berlin K, Miller JR, Bergman NH, Phillippy AM. 2017. Canu: scalable and accurate long-read assembly via adaptive k-mer weighting and repeat separation. Genome Res 27:722-736.
87. Altschul SF, Gish W, Miller W, Myers EW, Lipman DJ. 1990. Basic local alignment search tool. J Mol Biol 215:403-10.
88. Kitson E. 2018. Simple-Circularise. https://github.com/Kzra/Simple-Circularise. Accessed September 19, 2019.
89. Chaumeil PA, Mussig AJ, Hugenholtz P, Parks DH. 2019. GTDB-Tk: a toolkit to classify genomes with the Genome Taxonomy Database. Bioinformatics doi:10.1093/bioinformatics/btz848.
90. Seemann T. 2014. Prokka: rapid prokaryotic genome annotation. Bioinformatics 30:2068-9.
91. Schmieder R, Lim YW, Rohwer F, Edwards R. 2010. TagCleaner: Identification and removal of tag sequences from genomic and metagenomic datasets. BMC Bioinformatics 11:341.
92. Callahan BJ, McMurdie PJ, Rosen MJ, Han AW, Johnson AJ, Holmes SP. 2016. DADA2: High-resolution sample inference from Illumina amplicon data. Nat Methods 13:581-3.
93. Edgar RC, Flyvbjerg H. 2015. Error filtering, pair assembly and error correction for next-generation sequencing reads. Bioinformatics 31:3476-82.
94. Quast C, Pruesse E, Yilmaz P, Gerken J, Schweer T, Yarza P, Peplies J, Glockner FO. 2013. The SILVA ribosomal RNA gene database project: improved data processing and web-based tools. Nucleic acids research 41:D590-6.
95. Callahan BJ, Wong J, Heiner C, Oh S, Theriot CM, Gulati AS, McGill SK, Dougherty MK. 2019. High-throughput amplicon sequencing of the full-length 16S rRNA gene with single-nucleotide resolution. Nucleic Acids Res 47:e103.
96. Parks DH, Chuvochina M, Waite DW, Rinke C, Skarshewski A, Chaumeil PA, Hugenholtz P. 2018. A standardized bacterial taxonomy based on genome phylogeny substantially revises the tree of life. Nat Biotechnol 36:996-1004.
97. Dec 28 2013. D1. The SILVA and "All-species Living Tree Project (LTP)" taxonomic frameworks. Nucleic Acids Res, 42.D643-D648. https://academic.oup.com/nar/article-lookup/doi/10.1093/nar/gkt1209.
98. Aug 10 2007. 16. Naive Bayesian Classifier for Rapid Assignment of rRNA Sequences into the New Bacterial Taxonomy. Applied and Environmental Microbiology, 73.5261-5267. http://aem.asm.org/cgi/doi/10.1128/AEM.00062-07.
99. Anonymous. 2019. NCBI 16S RefSeq Nucleotide sequence records.
100. Cole JR, Wang Q, Cardenas E, Fish J, Chai B, Farris RJ, Kulam-Syed-Mohideen AS, McGarrell DM, Marsh T, Garrity GM, Tiedje JM. 2009. The Ribosomal Database Project: improved alignments and new tools for rRNA analysis. Nucleic Acids Res 37:D141-5.
101. Ritari J, Salojarvi J, Lahti L, de Vos WM. 2015. Improved taxonomic assignment of human intestinal 16S rRNA sequences by a dedicated reference database. BMC Genomics 16:1056.
102. Oksanen J, Blanchet FG, Kindt R, Legendre P, Minchin PR, O'Hara RB, Simpson GL, Solymos P, Stevens MHH, Wagner H. 2011. vegan: Community Ecology Package. R package version 20-2.

103. Maechler M. 2016. cluster: "Finding Groups in Data": Cluster Analysis Extended Rousseeuw et al. Accessed Feb 7.
104. Stamatakis A. 2014. RAxML version 8: a tool for phylogenetic analysis and post-analysis of large phylogenies. Bioinformatics 30:1312-3.
105. McMurdie PJ, Holmes S. 2013. phyloseq: an R package for reproducible interactive analysis and graphics of microbiome census data. PLoS One 8:e61217.
106. Bokulich NA, Dillon MR, Zhang Y, Rideout JR, Bolyen E, Li H, Albert PS, Caporaso JG. 2018. q2-longitudinal: Longitudinal and Paired-Sample Analyses of Microbiome Data. mSystems 3.
107. Grtton A, Herbrich R, Smola A, Bousquet O, Scholkopf B. 2005. Kernel Methods for Measuring Independence. Journal of Machine Learning Research 6:2075-2129.
108. Plummer M. 2011. rjags: Bayesian graphical models using MCMC, http://CRAN.R-project.org/package=rjags.
109. Team RDC. 2012. R: A Language and Environment for Statistical Computing, Vienna, Austria.
110. Faulkner JR, Minin, V. 2018. Locally adaptive smoothing with Markov random fields and shrinkage priors. Bayesian Analysis 13:225-252.
111. Team SD. 2018. RStan: the R interface to Stan. R package version 2.17.3.
112. Frank E, Hall M, Trigg L, Holmes G, Witten IH. 2004. Data mining in bioinformatics using Weka. Bioinformatics 20:2479-81.
113. Hall M, Frank E, Holmes G, Pfahringer B, Reutemann P, Witten IH. 2009. The WEKA Data Mining Software: An Update. SIGKDD Explorations 11.
114. Muret EA. 2020. An anvi'o workflow for microbial pangenomics. http://merenlab.org/2016/11/08/pangenomics-v2/. Accessed
115. Storey J, Bass A, Dabney A, Robinson D. 2020. qvalue: Q-value estimation for false discovery rate control. R package version 2.22.0, http://github.com/jdstorey/qvalue.
116. Rotmistrovsky K, Agarwala R. 2011. BMTagger: Best Match Tagger for removing human reads from metagenomics datasets. NCBI/NLM, National Institutes of Health.
117. Church DM, Schneider VA, Graves T, Auger K, Cunningham F, Bouk N, Chen HC, Agarwala R, McLaren WM, Ritchie GR, Albracht D, Kremitzki M, Rock S, Kotkiewicz H, Kremitzki C, Wollam A, Trani L, Fulton L, Fulton R, Matthews L, Whitehead S, Chow W, Torrance J, Dunn M, Harden G, Threadgold G, Wood J, Collins J, Heath P, Griffiths G, Pelan S, Grafham D, Eichler EE, Weinstock G, Mardis ER, Wilson RK, Howe K, Flicek P, Hubbard T. 2011. Modernizing reference genome assemblies. PLoS biology 9:e1001091.
118. Langmead B, Trapnell C, Pop M, Salzberg SL. 2009. Ultrafast and memory-efficient alignment of short DNA sequences to the human genome. Genome biology 10:R25.
119. Bolger AM, Lohse M, Usadel B. 2014. Trimmomatic: a flexible trimmer for Illumina sequence data. Bioinformatics 30:2114-20.
120. Segata N, Waldron L, Ballarini A, Narasimhan V, Jousson O, Huttenhower C. 2012. Metagenomic microbial community profiling using unique clade-specific marker genes. Nature methods 9:811-4.
121. Bankevich A, Nurk S, Antipov D, Gurevich AA, Dvorkin M, Kulikov AS, Lesin VM, Nikolenko SI, Pham S, Prjibelski AD, Pyshkin AV, Sirotkin AV, Vyahhi N, Tesler G,

Alekseyev MA, Pevzner PA. 2012. SPAdes: a new genome assembly algorithm and its applications to single-cell sequencing. J Comput Biol 19:455-77.

122. Kang DD, Froula J, Egan R, Wang Z. 2015. MetaBAT, an efficient tool for accurately reconstructing single genomes from complex microbial communities. PeerJ 3:e1165.

123. Huerta-Cepas J, Szklarczyk D, Forslund K, Cook H, Heller D, Walter MC, Rattei T, Mende DR, Sunagawa S, Kuhn M, Jensen LJ, von Mering C, Bork P. 2016. eggNOG 4.5: a hierarchical orthology framework with improved functional annotations for eukaryotic, prokaryotic and viral sequences. Nucleic Acids Res 44:D286-93.

124. Kanehisa M, Goto S, Sato Y, Furumichi M, Tanabe M. 2012. KEGG for integration and interpretation of large-scale molecular data sets. Nucleic acids research 40:D109-14.

125. Finn RD, Coggill P, Eberhardt RY, Eddy SR, Mistry J, Mitchell AL, Potter SC, Punta M, Qureshi M, Sangrador-Vegas A, Salazar GA, Tate J, Bateman A. 2016. The Pfam protein families database: towards a more sustainable future. Nucleic Acids Res 44:D279-85.

126. Lombard V, Golaconda Ramulu H, Drula E, Coutinho PM, Henrissat B. 2014. The carbohydrate-active enzymes database (CAZy) in 2013. Nucleic Acids Res 42:D490-5.

127. Cantarel BL, Coutinho PM, Rancurel C, Bernard T, Lombard V, Henrissat B. 2009. The Carbohydrate-Active EnZymes database (CAZy): an expert resource for Glycogenomics. Nucleic Acids Res 37:D233-8.

128. Delmont TO, Eren AM. 2018. Linking pangenomes and metagenomes: the Prochlorococcus metapangenome. PeerJ 6:e4320.

129. Enright AJ, Van Dongen S, Ouzounis CA. 2002. An efficient algorithm for large-scale detection of protein families. Nucleic Acids Res 30:1575-84.

130. Edgar RC. 2004. MUSCLE: multiple sequence alignment with high accuracy and high throughput. Nucleic Acids Res 32:1792-7.

131. Pierce NT, Irber L, Reiter T, Brooks P, Brown CT. 2019. Large-scale sequence comparisons with sourmash. F1000Res 8:1006.

132. Darling AE, Mau B, Perna NT. 2010. progressiveMauve: multiple genome alignment with gene gain, loss and rearrangement. PloS one 5:e11147.

133. Rissman AI, Mau B, Biehl BS, Darling AE, Glasner JD, Perna NT. 2009. Reordering contigs of draft genomes using the Mauve aligner. Bioinformatics 25:2071-3.

FIGURES AND TABLES LEGENDS

FIG 1 Study design. *Demographic, clinical, and nutritional information was collected for each enrolled preterm neonate. Inclusion: 24^{0}-32^{6} weeks, <4d age. Exclusion criteria include nonviable or planned withdrawal of care, severe asphyxia, chromosome abnormalities, cyanotic congenital heart disease, intestinal atresia or perforation, abdominal wall defects, significant GI dysfunction, galactosemia or other forms of galactose intolerance. **Intestinal permeability was measured using urine non-metabolized sugar probes lactulose and rhamnose day 7-10 post-birth. ***Stool specimens were collected daily at every stooling event, stored in storage buffer and archived in -80°C.

FIG 2 Pie chart of feeding types of the preterm infant population in this study (A). Abbr: MOM: mother's breastmilk feeding; PHDM: pasteurized human donor's milk. Boxplot of the IP measurement grouped by feeding types (B). Correlation between intestinal permeability and the cumulative amount of mom's own breastmilk feeding (ml/kg) for a total of 113 enrolled preterm infants $24^{0/7}$-$32^{6/7}$ weeks of gestation were enrolled (C). IP was calculated using the ratio of urine Lactulose (La) and Rhamnose (Rh), low and high IP was defined by a La/Rh >0.05 or ≤0.05, respectively. The total amount of mom's own breastmilk feeding was calculated as sum of the daily amount of milk intake per kilogram bodyweight until d7-10 when the IP was measured. Initial feed was calculated based on 10 ml/kg expressed breast milk between the first and fourth day of life depending on clinical stability. After 3-5 days initial feeds, feedings were advanced by 20 ml/kg/d until 100 ml/kg/d was reached. Plotted are interquartile ranges (IQRs, boxes),

1196 medians (line in box), and mean (diamond). Significance value was calculated using
1197 Wilcoxon rank sum test. Star sign (*) denotes the level of significance. “NS” denotes
1198 non-significant.
1199
1200 **FIG 3** Microbial biomarkers and breastmilk feeding in early preterm subjects with high
1201 and low IP. Abundance of bacterial groups stratified by postmenstrual age at study day
1202 7-10. It indicates the Actinobacteria (*Bifidobacterium*) and Clostridia (Clostridiales) that
1203 were mainly observed in low IP subjects but not in high IP subject (red) (A). The
1204 abundance values of read count for each ASVs are stacked in order from greatest to
1205 least, separate by a horizontal line. Boxplot of the *Bifidobacterium* relative abundance
1206 and cumulative amount of mom’s breastmilk feeding (ml/kg) during the first 7-10
1207 postnatal days in subjects with high or low IP (B). IP was calculated using the ratio of
1208 urine Lactulose (La) and Rhamnose (Rh), low and high IP defined by a La/Rh >0.05 or
1209 ≤0.05, respectively. Plotted are interquartile ranges (IQRs, boxes), medians (line in box),
1210 and mean (diamond). Significance value was calculated using Wilcoxon rank sum test.
1211 Star sign (*) denotes the level of significance. “NS” denotes non-significant. Volatility
1212 plot to demonstrate the fluctuation of microbial community diversity (C) (characterized
1213 as Shannon diversity index) and *Bifidobacterium* diversity over MOM feeding volume in
1214 high or low IP groups (D). Plot was generated in QIIME (2019.10 vers) (106). Non-
1215 overlapping of the vertical error bar at each measuring point was considered
1216 significantly different. Temporal characterization of intestinal microbiota of early preterm
1217 infants to profile changes over the first 21 days post-birth (E). Taxonomic profile was
1218 generated using 16S rRNA gene sequencing. Community type is shown in Fig. S3

heatmap clusters. The dates when IP was measured, MOM, PHDM, formula feeding day, antibiotics administration are shown in the plot. Each circle is sized proportionally the feeding volume. Abbr: MOM: mother's own breastmilk feeding; PHDM: pasteurized human donor's milk.

FIG 4 Phylogenetic tree constructed using 81 unique, full-length 16S rRNA gene ASV sequences of *Bifidobacterium* (A). ANI clustering of full-length 16S rRNA gene sequences (B). Phylogenetic tree of *Bifidobacterium* ASVs in stool microbiota of cohort (C). All full-length 16S rRNA genes assigned to *Bifidobacterium* were used in the analyses. Color denotes individual subjects.

FIG 5 Illustration of the mature and immature intestinal barrier in neonates. Peristalsis (reduced intestinal motility), maldigestion of nutrient sources and a compromised gut barrier may render the mucosa susceptible to invasion by the opportunistic pathogens in gut environment. The resulting imbalance between epithelial cell injury and repair leads to a vicious cycle of maldigestion, bacterial invasion, immune activation and uncontrolled inflammation. Illustration not drawn to scale. Created with BioRender.com.

TABLE 1 Study cohort demographics and clinical variables stratified by intestinal permeability (IP) category

TABLE 2 Odds ratio for factors associated with Low IP Adjusted for postmenstrual age (PMA) and birth weight (BW)

Supplementary Figures and Table legends

FIG S1 Intestinal permeability (IP) and cohort clinical information. **A**) Notched boxplot of IP for early preterm subjects (GA < 33 weeks gestation). Subjects were categorized by IP-measuring day between study day 7-10 and by IP category. The top and bottom of the box are the lower and upper quartiles, and the band near the middle of the box represents the median. The width of the notch can be used to roughly compare two distributions. For example, two distributions without overlapping notch regions can be roughly considered as being significantly different from each other (1). IP was measured by non-metabolized sugar probes lactulose and rhamnose. High IP was defined by a La/Rh ratio >0.05, as validated and applied previously (2). **B**) Correlation matrices visualization of the subjects' physiological age. R package Correlograms (corrgram) were used to visualize the correlation matrices. Pearson correlation method used to calculate correlation. **Abbr**: PMA at dosing: postmenstrual age calculated at the dosing day when IP was measured; PMA at enrollment: postmenstrual age at enrollment day taken place within 1-4 days post-birth; GA: gestational age; BW: birthweight; body weight at dosing: subject weight measured at the dosing day when IP was measured.

FIG S2 Phylogenetic tree of all ASVs of full-length 16S rRNA gene sequenced on Pacific Biosciences Sequel II platform. Package raxml (v8.0.0) (3) was used to construct the phylogeny, Phyloseq R package (4) was used to display the phylogeny.

FIG S3 Heatmap of the 50 most abundant intestinal bacterial taxa relative abundance in samples collected from 113 preterm infants enrolled in the study. The fecal microbiota was characterized by high-throughput sequencing of the V3-V4 variable regions of 16S rRNA genes. Ward linkage clustering was used to cluster samples based on their Jensen-Shannon distance calculated in vegan package in R (5). The number of clusters was validated using gap statistics implemented in the *cluster* package in R (6) by calculating the goodness of clustering measure.

FIG S4 Information on bifidobacterial abundance and intestinal permeability (IP). **A**) Relative abundance of bifidobacterial bacterial groups stratified by feeding types.

Phyloseq R package (v1.38.0) (4) was used to generate the barplot. **B**) The relative abundance of *B. breve* between high-IP and low-IP groups. Dependence between **C**) IP or **D**) MOM feeding dose and the log relative abundance of *B. breve*. An adaptive spline logistic regression model implemented in spmrf R package (7) was applied to the phylotypes present in at least 15% of all samples. Bayesian goodness-of-fit p-value implemented in R package rstan (8) was used to access the significance of the association between phylotypes and investigated factors.

FIG S5 Metapangenome of *Bifidobacterium breve*. The 26 *in-house B. breve* MAGs was supplemented with 107 published genomes (https://doi.org/10.6084/m9.figshare.19709917.v2 **A**) and our 4 *B. longum* MAGs was supplemented with 310 published genomes (https://doi.org/10.6084/m9.figshare.19709917.v2 **B**) for pangenome construction following pangenome workflow (9). *B. breve* pangenome was displayed using anvi'o *vers* 6.2 (10). BLASTP was used to compute ANI identity between all pairs of genes. Markov Cluster Algorithm (MCL) (11) was used to generate homologous gene clusters (HGCs). Amino acid sequences of each HGC were aligned using MUSCLE (12). HCG was assigned to core, accessory or dispensable according the hierarchical clustering of the gene clusters. Detail of each HGC was in https://doi.org/10.6084/m9.figshare.19709917.v2 **C**. Sourmash vers 3.3 (13) was used to compute Average nucleotide identity (ANI) across genomes. The source indicates the isolated origin of the genome, and genomes of the same subject are indicated in the same cohort.

FIG S6 The complete *B. breve* genome reconstructed in this study. Metagenomic sequencing of the two selected fecal samples was performed using the Pacific Bioscience Sequel II platform, followed by assembly using Canu v1.8 (14) and deconvolution using BLASTN of the assembly. This complete genome was 2.34M in size (https://doi.org/10.6084/m9.figshare.19709923.v1, https://doi.org/10.6084/m9.figshare.19723255.v1**C**), similar to median *B. breve*

genome size of 2.33M reported on NCBI. **A**) KEGG 2013-03-18 release (15) to characterize functional categories of *B. breve* XM1439. **B**) Circular genome display of *B. breve* XM1439, generated by BLAST Ring Image Generator (BRIG) (2011 June vers) (16). **C**) Genome alignment of *B. breve* genome 1439, 1437 using MAUVE (17) using *B. breve* DSM20213 as the reference genome.

TABLE S1. Clinical metadata of the 113 early preterm infant subjects used in this study.

TABLE S2. Dependence of demographic, obstetric, and neonatal characteristics with intestinal permeability (IP) using Hilbert-Schmidt Independence Criterion (HSIC) implemented in R package dHSIC.

TABLE S3. Taxonomic groups significantly associated with PMA, IP and MOM feeding volume. Zero-inflated negative binomial random effects (ZINBRE) models were used to compute significance level of association, which accounts for many zeros as well for correlations between samples from the same subject. All phylotypes detected in at least 15% samples were modeling using ZINBRE models. PMA, IP and MOM feeding volume were modeled as continuous value. **A**) Taxonomic groups associated with PMA, which was calculated as day of life after birth plus gestational age; **B**) Taxonomic groups associated with IP, measured at 7-10 days after birth; **C**) Taxonomic groups significantly associated with MOM feeding volume. **Abbr**: **MOM**: mother's own breastmilk feeding. **PMA**: postmenstrual age. **IP**: intestinal permeability.

TABLE S4. *Bifidobacterium* homologous gene clusters (HGCs) characterized to involved in human milk oligosaccharides assimilation. Genomes were annotated through annotative evidences from the nomenclature of the consortium for function glycomics, eggNOG (v4.5)(18), KEGG (FTP Release 2013-03-18)(15)), Pfam (v30.0)(19), CAZy (2014 release) (20, 21). Similarity searches were performed to previously annotated enzymes or transporter proteins based on the accession number listed in previous studies (22-24), using BLASTP similarity search and confirmed with the COG, Pfam and CAZy annotation evidence to ensure the integrity of the results. **A**) HGCs involved in extracellular enzymes and their homologs involved in extracellular cleavage of HMOs; **B**) HGCs characterized as family 1 solute binding proteins (F1SBP); **C**) HGCs involved in enzymes for catabolizing HMOs substrates intracellularly; **D**)

HGCs characterized as FHMO (Fucosylated Human Milk Oligosaccharide utilization cluster); **E**) HGCs involved in sialylated HMO substrates catabolism; **F**) HGCs involved in sulfatase catabolism activity.

SUPPLEMENTARY MATERIALS REFERENCES

1. McGill R, Tukey JW, Larsen WA. 1978. Variations of Box Plots. The American Statistician 32:12–16.
2. Saleem B, Okogbule-Wonodi AC, Fasano A, Magder LS, Ravel J, Kapoor S, Viscardi RM. 2017. Intestinal Barrier Maturation in Very Low Birthweight Infants: Relationship to Feeding and Antibiotic Exposure. J Pediatr 183:31-36 e1.
3. Stamatakis A. 2014. RAxML version 8: a tool for phylogenetic analysis and post-analysis of large phylogenies. Bioinformatics 30:1312-3.
4. McMurdie PJ, Holmes S. 2013. phyloseq: an R package for reproducible interactive analysis and graphics of microbiome census data. PLoS One 8:e61217.
5. Oksanen J, Blanchet FG, Kindt R, Legendre P, Minchin PR, O'Hara RB, Simpson GL, Solymos P, Stevens MHH, Wagner H. 2011. vegan: Community Ecology Package. R package version 20-2.
6. Maechler M. 2016. cluster: "Finding Groups in Data": Cluster Analysis Extended Rousseeuw et al. Accessed Feb 7.
7. Faulkner JR, Minin, V. 2018. Locally adaptive smoothing with Markov random fields and shrinkage priors. Bayesian Analysis 13:225-252.
8. Team SD. 2018. RStan: the R interface to Stan. R package version 2.17.3.
9. Muret EA. 2020. An anvi'o workflow for microbial pangenomics. http://merenlab.org/2016/11/08/pangenomics-v2/. Accessed
10. Delmont TO, Eren AM. 2018. Linking pangenomes and metagenomes: the Prochlorococcus metapangenome. PeerJ 6:e4320.
11. Enright AJ, Van Dongen S, Ouzounis CA. 2002. An efficient algorithm for large-scale detection of protein families. Nucleic Acids Res 30:1575-84.
12. Edgar RC. 2004. MUSCLE: multiple sequence alignment with high accuracy and high throughput. Nucleic Acids Res 32:1792-7.
13. Pierce NT, Irber L, Reiter T, Brooks P, Brown CT. 2019. Large-scale sequence comparisons with sourmash. F1000Res 8:1006.
14. Koren S, Walenz BP, Berlin K, Miller JR, Bergman NH, Phillippy AM. 2017. Canu: scalable and accurate long-read assembly via adaptive k-mer weighting and repeat separation. Genome Res 27:722-736.
15. Kanehisa M, Goto S, Sato Y, Furumichi M, Tanabe M. 2012. KEGG for integration and interpretation of large-scale molecular data sets. Nucleic acids research 40:D109-14.
16. Alikhan NF, Petty NK, Ben Zakour NL, Beatson SA. 2011. BLAST Ring Image Generator (BRIG): simple prokaryote genome comparisons. BMC Genomics 12:402.
17. Rissman AI, Mau B, Biehl BS, Darling AE, Glasner JD, Perna NT. 2009. Reordering contigs of draft genomes using the Mauve aligner. Bioinformatics 25:2071-3.
18. Huerta-Cepas J, Szklarczyk D, Forslund K, Cook H, Heller D, Walter MC, Rattei T, Mende DR, Sunagawa S, Kuhn M, Jensen LJ, von Mering C, Bork P. 2016. eggNOG 4.5: a hierarchical orthology framework with improved functional annotations for eukaryotic, prokaryotic and viral sequences. Nucleic Acids Res 44:D286-93.

19. Finn RD, Coggill P, Eberhardt RY, Eddy SR, Mistry J, Mitchell AL, Potter SC, Punta M, Qureshi M, Sangrador-Vegas A, Salazar GA, Tate J, Bateman A. 2016. The Pfam protein families database: towards a more sustainable future. Nucleic Acids Res 44:D279-85.
20. Lombard V, Golaconda Ramulu H, Drula E, Coutinho PM, Henrissat B. 2014. The carbohydrate-active enzymes database (CAZy) in 2013. Nucleic Acids Res 42:D490-5.
21. Cantarel BL, Coutinho PM, Rancurel C, Bernard T, Lombard V, Henrissat B. 2009. The Carbohydrate-Active EnZymes database (CAZy): an expert resource for Glycogenomics. Nucleic Acids Res 37:D233-8.
22. Sakanaka M, Gotoh A, Yoshida K, Odamaki T, Koguchi H, Xiao JZ, Kitaoka M, Katayama T. 2019. Varied Pathways of Infant Gut-Associated Bifidobacterium to Assimilate Human Milk Oligosaccharides: Prevalence of the Gene Set and Its Correlation with Bifidobacteria-Rich Microbiota Formation. Nutrients 12.
23. Odamaki T, Horigome A, Sugahara H, Hashikura N, Minami J, Xiao JZ, Abe F. 2015. Comparative Genomics Revealed Genetic Diversity and Species/Strain-Level Differences in Carbohydrate Metabolism of Three Probiotic Bifidobacterial Species. Int J Genomics 2015:567809.
24. Ruiz-Moyano S, Totten SM, Garrido DA, Smilowitz JT, German JB, Lebrilla CB, Mills DA. 2013. Variation in consumption of human milk oligosaccharides by infant gut-associated strains of Bifidobacterium breve. Appl Environ Microbiol 79:6040-9.

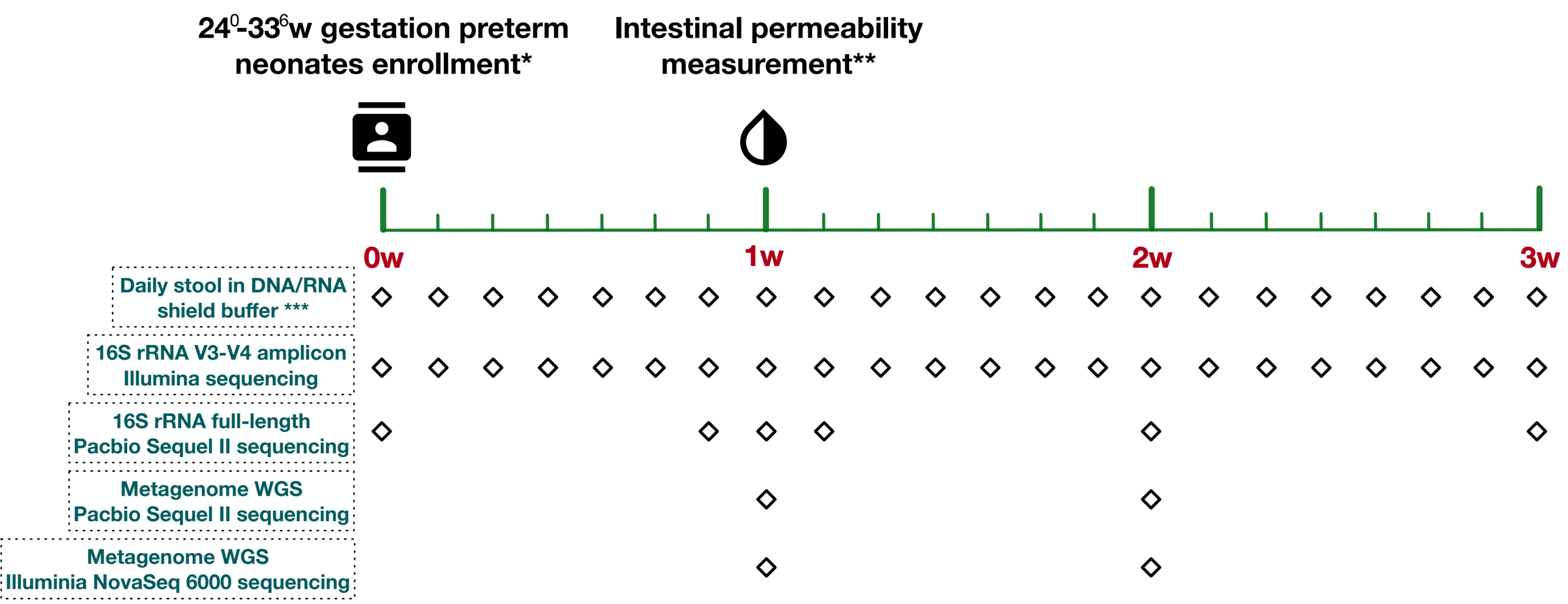

*Geographical, clinical, and nutritional information was collected for each enrolled preterm neonate. Inclusion: 24^0-32^6 weeks, <4d age
Exclusion: nonviable or planned withdrawal of care, severe asphyxia, chromosome abnormalities, cyanotic congenital heart disease, intestinal atresia or perforation, abdominal wall defects, significant GI dysfunction, galactosemia or other forms of galactose intolerance

**Intestinal permeability was measured using urine non-metabolized sugar probes lactulose and rhamnose during the first 7-10 days of life

***Stool specimen was collected daily at every stooling event

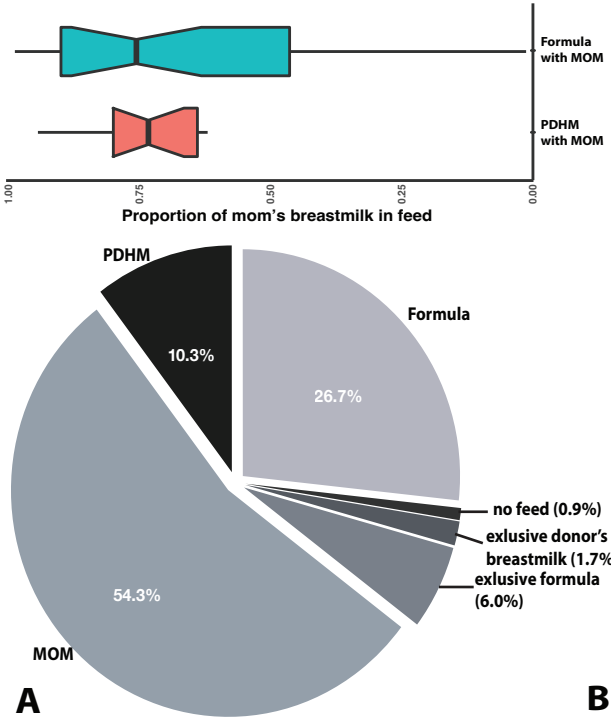
Formula with MOM
PDHM with MOM
1.00
0.75
0.50
0.25
0.00
Proportion of mom's breastmilk in feed
PDHM
Formula
10.3%
26.7%
no feed (0.9%)
exlusive donor's breastmilk (1.7%)
exlusive formula (6.0%)
54.3%
MOM
A

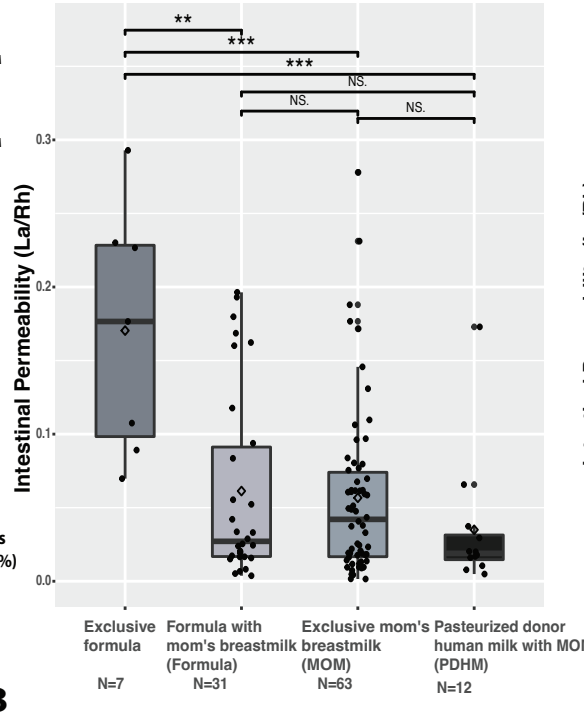
**
***
***
NS.
NS.
NS.
Intestinal Permeability (La/Rh)
0.3
0.2
0.1
0.0
Exclusive formula
N=7
Formula with mom's breastmilk (Formula)
N=31
Exclusive mom's breastmilk (MOM)
N=63
Pasteurized donor human milk with MOM (PDHM)
N=12
B

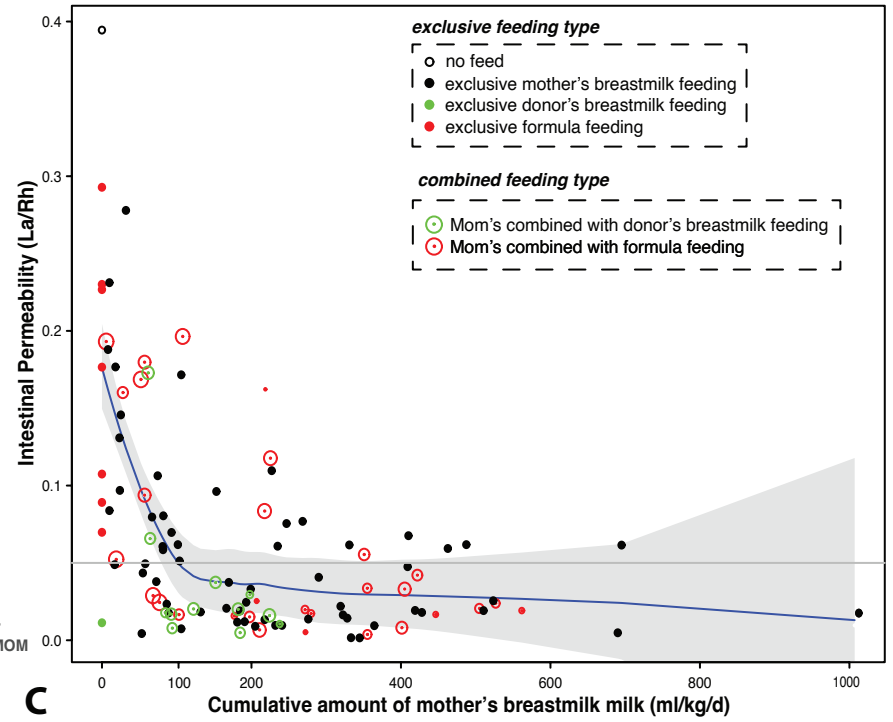
exclusive feeding type
no feed
exclusive mother's breastmilk feeding
exclusive donor's breastmilk feeding
exclusive formula feeding
combined feeding type
Mom's combined with donor's breastmilk feeding
Mom's combined with formula feeding
Intestinal Permeability (La/Rh)
0.4
0.3
0.2
0.1
0.0
0
100
200
400
600
800
1000
Cumulative amount of mother's breastmilk milk (ml/kg/d)
C

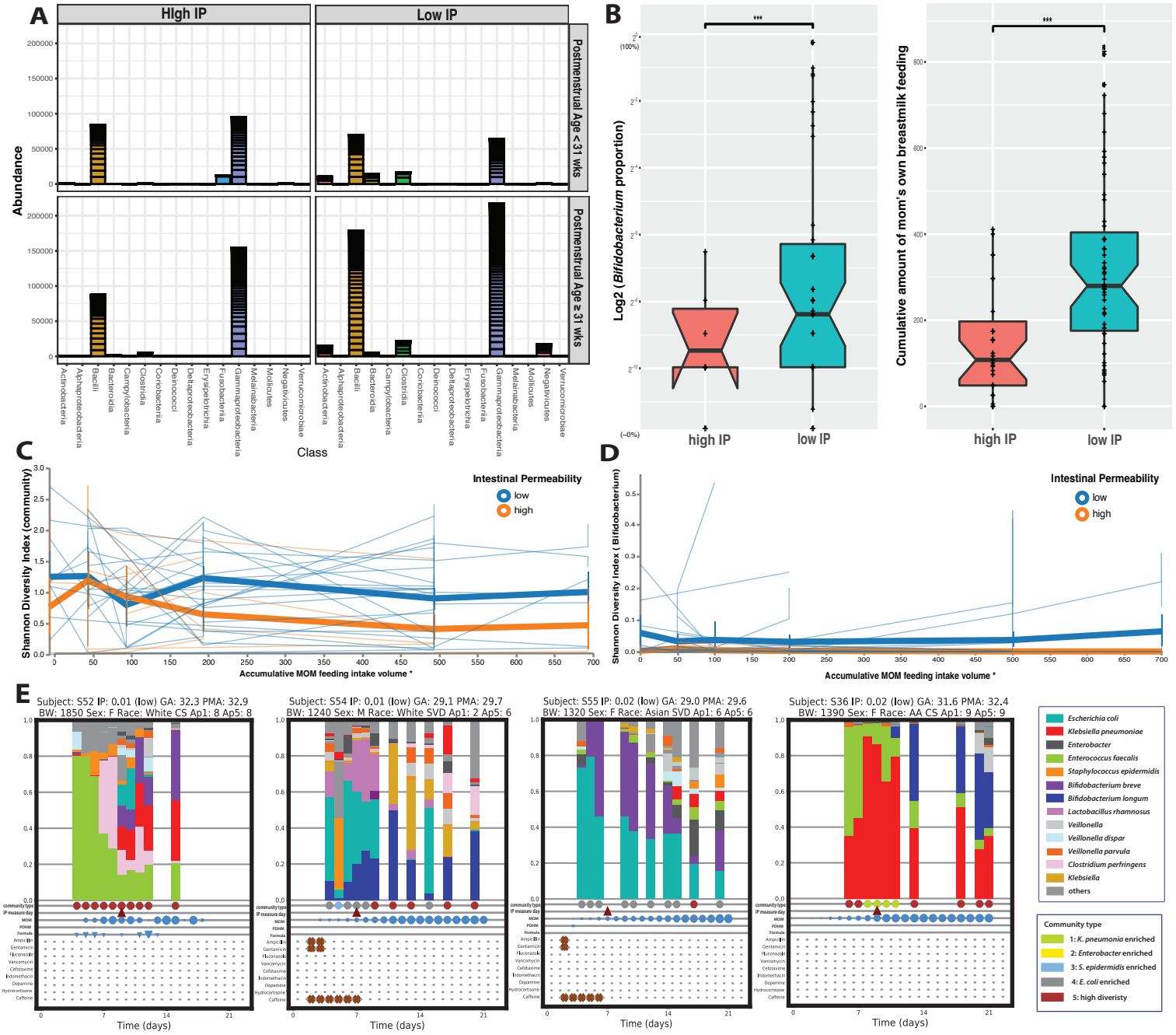

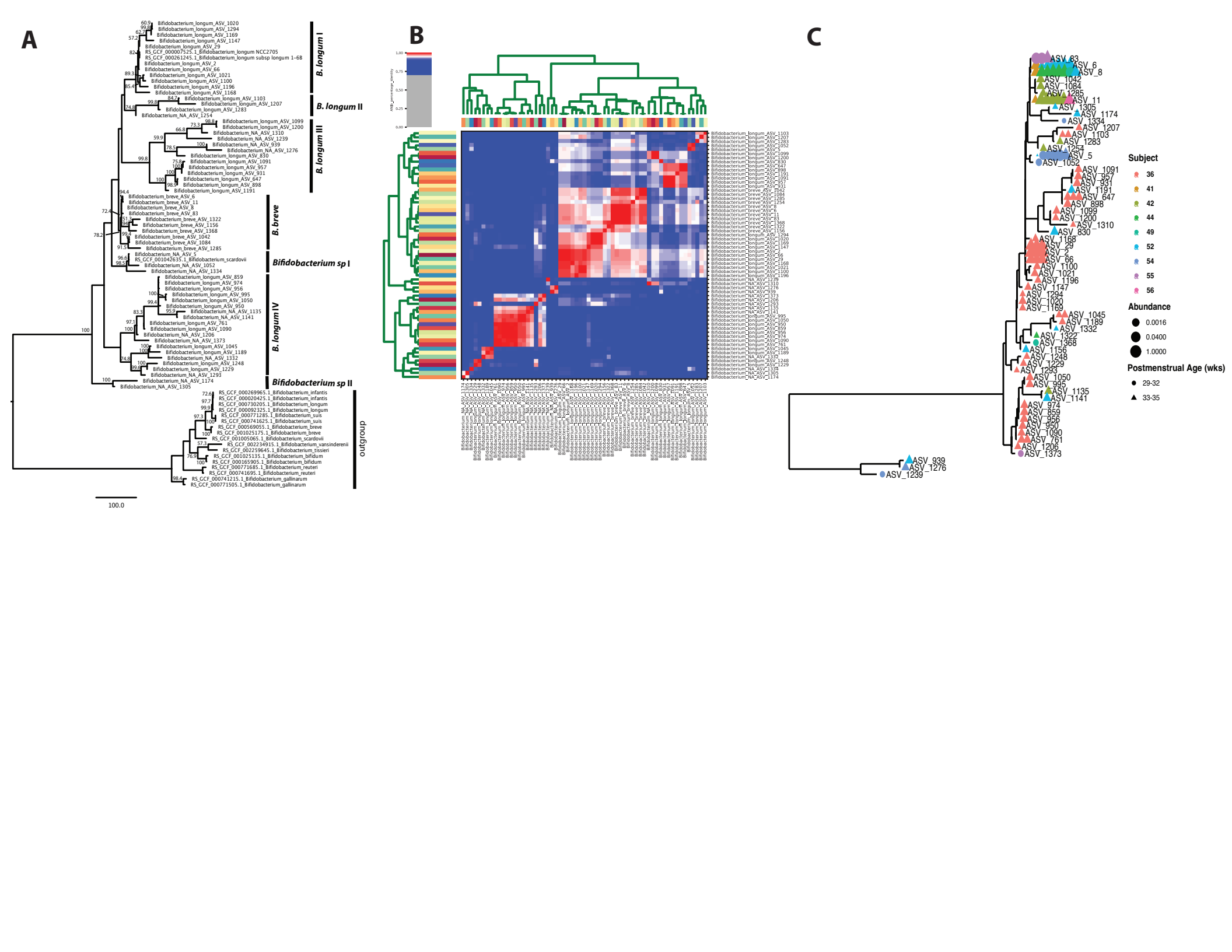
A
B
C
B. longum I
B. longum II
B. longum III
B. breve
Bifidobacterium sp I
B. longum IV
Bifidobacterium sp II
outgroup
100.0
Subject
Abundance
Postmenstrual Age (wks)

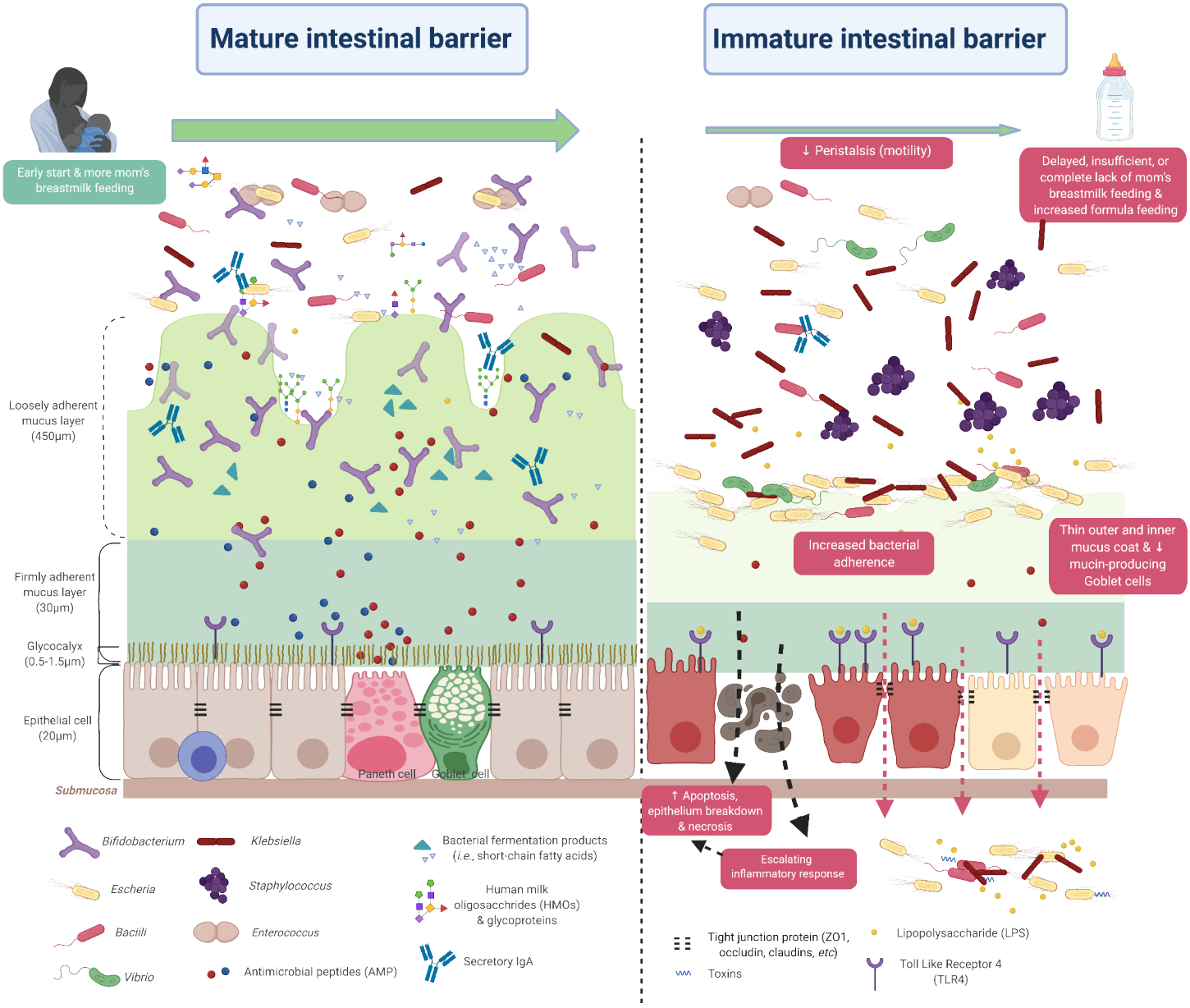

TABLE 1 Study cohort demographics and clinical variables stratified by intestinal permeability (IP) category

Variables	Total cohort (N=113) (N (%) / mean ± SD)	High IP (n=48) (n (%) / mean ± SD)	Low IP (n=65) (n (%) / mean ± SD)	p-value*
Sex				0.28
Male	61 (54.0)	24 (50.0)	37 (57.0)	
Female	52 (46.0)	24 (50.0)	28 (43.1)	
Race				
White	42 (37.2)	18 (37.5)	24 (37.0)	1.00
African American	63 (55.8)	30 (62.5)	33 (50.8)	0.25
Other	8 (7.1)	0	8 (12.3)	0.02
Birth weight (gram)	1377.8 ± 415.2	1237.3 ± 378.1	1496.5 ± 403.0	<0.01
VLBW (<1,500 g)	66 (58.4)	32 (66.7)	34 (52.3)	0.18
Gestational age (wks)	29.8 ± 2.3	29.0 ± 2.3	30.5 ± 2.1	<0.01
Early GA (≤28 wks)	28 (24.8)	18 (37.5)	10 (15.4)	<0.01
Postmenstrual age (wks)	31.1 ± 2.3	30.3 ± 2.3	31.7 ± 2.1	<0.01
Early PMA (<31 wks)	41 (36.3)	23 (47.9)	18 (27.7)	0.03
Caesarean delivery	77 (68.1)	37 (77.1)	40 (61.5)	0.10
PPROM	36 (31.9)	15 (31.3)	21 (32.3)	1.00
Preeclampsia	25 (22.1)	11 (23.0)	14 (21.5)	1.00
Antenatal corticosteroids	106 (94.0)	46 (96.0)	60 (92.3)	0.70
Maternal antibiotics	69 (61.1)	30 (62.5)	39 (60.0)	0.85
APGAR Score at 1 min	5.8 ± 2.5	5.3 ±2.8	6.2 ± 2.1	0.04
APGAR Score at 5 min	7.7 ± 1.6	7.5 ± 1.9	7.9 ± 1.6	0.12
Antibiotic types				
Ampicillin received	64 (56.7)	30 (62.5)	34 (52.3)	0.33
Gentamycin received	56 (49.6)	25 (52.1)	31 (47.7)	0.70
Vancomycin received	8 (7.1)	6 (12.5)	2 (3.1)	0.07
Cefotaxime received	9 (8.0)	6 (12.5)	3 (4.6)	0.16
Received at least one antibiotic vs. no antibiotics[a]	68 (60.2)	33 (68.8)	35 (53.9)	0.12
Antibiotics days received[a]				
≤ 3 days	83 (73.5)	30 (62.5)	53 (81.5)	0.03
> 3 days	30 (26.6)	18 (37.5)	12 (18.5)	
Days received MBM[a]				
< 4 days	26 (23.0)	20 (41.7)	6 (9.2)	< 0.01
≥ 4 days	87 (77.0)	28 (58.3)	59 (90.8)	
Feeding duration (number days)[a]				
Mother's own breast milk	4.8 ± 2.3	4 ± 2.7	5.5 ± 1.5	<0.01
Formula	1.3 ± 2.3	2 ± 2.7	0.8 ± 1.6	0.02
Feeding intake volume received[a]				
Mother's own breast milk	200.8 ± 178.8	123.4 ± 154.2	263.0 ± 175.6	< 0.01
Formula	61.7 ± 146.7	99.8 ± 194.7	32.8 ± 91.2	0.03

[a]Variable measured during the time-period starting from enrollment day (within 1 to 4 days after birth depending on clinical stability) until the day when IP was measured (day 8±2 post-birth).

TABLE 2 Odds ratio for factors associated with Low IP Adjusted for postmenstrual age (PMA) and birth weight (BW)[a]

	OR	95% CI	p-value[d]	Adjusted OR[c]	95% CI	p-value[d]
Duration of antibiotics use[b]						
≤ 3 days	2.65	1.12, 6.25	0.02	1.56	0.58, 4.16	0.37
> 3 days	1.0 (Ref)			1.0 (Ref)		
Duration of MOM feeding[b]						
≥ 4 days	7.04	2.5, 19.6	<0.01	10.30	3.21, 33.33	<0.01
< 4 days	1.0 (Ref)			1.0 (Ref)		

[a]Fisher's exact test was used to calculate p value for categorical variable. Student's t-test was used for continuous variables (BW, GA, PMA, APGAR score at 1 minute and 5 minutes). IP was calculated as the ratio of urine Lactulose (La) and Rhamnose (Rh) and La/ Rh < 0.05 was defined as low IP.
[b]Variable measured during the time-period starting from enrollment day (within 1 to 4 days after birth depending on clinical stability) until the day when IP was measured (day 8±2 post-birth).
[c]Adjusted OR model includes PMA and BW.
[d]p-value calculated using logistic regression.

ABBR: IP, Intestinal Permeability; PPROM, Premature Preterm Rupture of Membranes; BW: Birth Weight; VLBW, Very Low Birth Weight; MOM, Mothers own breastmilk; GA, Gestational Age; PMA, Postmenstrual Age; OR, Odds ratio; CI, confidence interval